# The leukocyte non-coding RNA landscape in critically ill patients with sepsis

Brendon P. Scicluna[1,2,*], Fabrice Uhel[1], Lonneke A. van Vught[1], Maryse A. Wiewel[1], Arie J. Hoogendijk[1], Ingelore Baessman[3], Marek Franitza[3], Peter Nürnberg[3,4], Janneke Horn[5], Olaf L. Cremer[6], Marc J. Bonten[7,8], Marcus J. Schultz[5], Tom van der Poll[1,9], MARS consortium.

Author affiliations:
[1]Amsterdam UMC, University of Amsterdam, Center for Experimental Molecular Medicine, Amsterdam Infection & Immunity, Amsterdam, the Netherlands.
[2]Amsterdam UMC, University of Amsterdam, Department of Clinical Epidemiology, Biostatistics and Bioinformatics, Amsterdam, the Netherlands.
[3]Cologne Center for Genomics, University of Cologne, Cologne, Germany.
[4]Center for Molecular Medicine Cologne, University of Cologne, Cologne, Germany.
[5]Amsterdam UMC, University of Amsterdam, Department of Intensive Care Medicine, University of Amsterdam, Amsterdam, the Netherlands.
[6]Department of Intensive Care, University Medical Center Utrecht, Utrecht, the Netherlands.
[7]Department of Medical Microbiology, University Medical Center Utrecht, Utrecht, the Netherlands.
[8]Julius Center for Health Sciences and Primary Care, University Medical Center Utrecht, Utrecht, the Netherlands.
[9]Amsterdam UMC, University of Amsterdam, Division of Infectious Diseases, Amsterdam, the Netherlands.

* Corresponding author: Brendon P. Scicluna, Amsterdam UMC, Univ. of Amsterdam, Center for Experimental Molecular Medicine and Department of Clinical Epidemiology, Biostatistics, and Bioinformatics, Amsterdam Infection & Immunity Institute, Room G2-105, Academic Medical Center, Meibergdreef 9, 1105AZ Amsterdam, the Netherlands. Email: b.scicluna@amc.uva.nl. Telephone: +31 20 566 7062. Fax: +31 20 697 7192.

**Abstract**

The extent of non-coding RNA alterations in patients with sepsis and their relationship to clinical characteristics, soluble mediators of the host response to infection, as well as an advocated *in vivo* model of acute systemic inflammation is unknown. Here, we obtained whole blood from 156 patients with sepsis and 82 healthy subjects among whom eight were challenged with lipopolysaccharide in a clinically controlled setting (human endotoxemia). Via next-generation microarray analysis of leukocyte RNA we found long non-coding RNA and, to a lesser extent small non-coding RNA, were significantly altered in sepsis relative to health. Long non-coding RNA expression, but not small non-coding RNA, were largely recapitulated in human endotoxemia. Integrating RNA profiles and plasma protein levels revealed known as well as previously unobserved pathways, including non-sensory olfactory receptor activity. We provide a benchmark dissection of the blood leukocyte "regulome" that can facilitate prioritization of future functional studies.

## Introduction

Sepsis is a multifaceted syndrome that develops as the consequence of an abnormal host response to infection leading to organ failure and high risk of death.[1, 2] It is estimated that 2-5 million deaths worldwide are attributable to sepsis.[3] Despite empirical antimicrobial therapy and advances in intensive care, it is expected that sepsis will remain a major healthcare problem. As such, sepsis has been recognized as a global health priority in 2017 by the World Health Assembly and WHO.[4] In spite of more than 100 clinical trials having evaluated drugs targeting specific components of the host response to infection,[5] no specific treatment for sepsis has been approved.[1, 2] This argues for a deeper understanding of sepsis immunopathology to identify veritable drug targets.[5, 6]

Protein-coding RNA expression profiling of blood leukocytes from sepsis patients has helped to broaden our understanding of sepsis immunopathology,[7] for example, by unmasking defects in leukocyte energy metabolism of sepsis patients,[8] and by classifying sepsis patients as transcriptomic endotypes with prognostic and pathophysiological value.[9-11] From fruit flies to man, the protein-coding part of genomes from different species is remarkably similar in numbers and functions,[12] which suggests that numerous aspects of complex biology in eukaryotes might stem from non-protein-coding regions of the genome. The increase in genomic coverage of tiled microarrays and massive cDNA sequencing undertaken by the Functional Annotation of the Mammalian genome (FANTOM) consortium revealed pervasive transcription outside of the known gene loci.[13, 14] Moreover, such studies facilitated the demonstration that non-coding RNAs were under negative evolutionary selection, which implied functionality rather than plain "transcriptional noise".[15] Indeed, a substantial proportion of non-coding RNA, by general convention defined as long (>200 nucleotides) or small (<200 nucleotides) non-coding RNAs, yields clear phenotypic effects in both *in vitro* and *in vivo* functional studies.[16-19] Ever-

growing numbers of small non-coding RNAs, for example micro (mi)RNAs (20-24 nucleotides), or long non-coding RNAs such as long intergenic non-coding (linc)RNAs, have been linked to human diseases.[20, 21] An important aspect of non-coding RNAs is their capacity for precise regulation of cellular biological processes via epigenetic mechanisms, including complex immune system processes.[22-24]

Knowledge of the non-coding RNA landscape in patients with sepsis is limited. Here, we report a comprehensive screen of non-coding RNA expression patterns in blood leukocytes of patients with sepsis and their relation to clinical characteristics and soluble mediators of the host response. In addition, by using a guilt-by-association approach we positioned non-coding RNAs in network modules encompassing protein-coding RNA reflecting distinct cellular biological pathways.

## Results

### Protein-coding and non-coding blood transcriptomes.

In order to build a comprehensive map of RNA expression in the context of sepsis, we evaluated protein-coding, long and small non-coding RNA expression in whole blood leukocytes from 156 sepsis patients and 82 healthy subjects (median age [Q1-Q3], 54 [42 – 60]; 26% male). Patient characteristics are tabulated in **Table 1 - source data 1**, causative pathogens in **Supplementary file 1**. Principal component (PC) analysis of the most abundant protein-coding RNAs (n=18,063) and long non-coding RNAs (n=16,087) showed clear partitioning of patients with sepsis distinct from healthy subjects (**Figure 1A**). In contrast, small non-coding RNAs (n=4949) showed only minimal separation between patients and healthy subjects. We observed similar patterns after calculating the molecular distance to health (MDTH)[25, 26] index, a measure of transcript-level expression perturbation relative to health, with significantly higher

MDTH indices in sepsis (**Figure 1B**). Notably, long non-coding RNA transcripts exhibited the broadest expression perturbations in healthy participants and sepsis patients, exemplified by the highest overall MDTH indices (**Figure 1B**).

Comparing sepsis patients to healthy subjects identified 15,097, 13,158 and 635 significantly altered (adjusted p-value<0.01) protein-coding, long and small non-coding RNAs, respectively (**Figure 1C**). Ingenuity pathway analysis of the significantly altered protein-coding RNA transcripts revealed associations to various canonical signaling pathways that included elevated pro- and anti-inflammatory pathways, cell cycle, DNA damage response and metabolic pathways (**Figure 1 - figure supplement 1**). Transcripts with reduced expression were predominantly associated to T helper cell activation, antigen presentation and B cell responses. Results on protein-coding RNA profiles are in agreement with previous reports from our and other groups.[7] LincRNAs, antisense and pseudogene RNA transcripts represented the most highly altered long non-coding RNA biotypes in sepsis relative to health (**Figure 1D**). Micro (mi)RNAs, stem loop RNAs and small nucleolar (sno)RNAs were the most abundant small non-coding RNA biotypes (**Figure 1E**).

## Protein-coding and non-coding blood transcriptomes, demographics and clinical characteristics

In order to understand inter-individual variation in RNA expression profiles, we set out to determine the contribution of demographics and clinical characteristics to protein-coding and non-coding RNA expression variation in sepsis patients (**Figure 2**), as well as healthy subjects. Using a variance partition (multivariable) approach,[27] differences in gender and age of healthy subjects explained 5%, 4% and 4% of the variation in protein-coding, long and small non-coding RNA expression, respectively (**Figure 2 - figure supplement 1A**). Specific transcripts had high

percentages of explainable variance, in particular long non-coding RNAs against gender. Not surprisingly, expression of long non-coding RNAs positioned on the X and Y chromosomes, for example *TXLNGY*, *LINC00278* and *XIST* had 98%, 97% and 94% of variance explained by gender, respectively (**Figure 2 - figure supplement 1B**). In sepsis patients, a multivariable model that incorporated demographics and common clinical characteristics, including APACHE IV, SOFA scores, shock and Charlson comorbidity indices, cumulatively explained 18%, 13% and 8% of protein-coding, long and small non-coding RNA expression variance, respectively (**Figure 2A**). Specifically, sepsis primary site of infection (lung or abdomen) and place of acquisition (community or hospital) explained the highest proportion of variation in protein-coding (6.7%) and long non-coding (4.4%) RNA expression (**Figure 2A**). Despite overall low proportions of variance explained, outlier RNA transcripts could be detected. For example, some specific transcripts demonstrated high individual explained variance against primary sepsis diagnosis, including protein-coding RNA encoding basic leucine zipper and W2 domains 1 (BZW1); long non-coding RNA SUMO2 pseudogene 1 (SUMO2P1); and small non-coding RNA miRNA hsa-miR-7855-5p (**Figure 2B**). Septic shock explained low proportions of variation in RNA expression (**Figure 2A**), and directly comparing patients with septic shock to patients without shock resulted in 837 and 80 significantly altered protein-coding and long non-coding RNA, respectively (**Figure 2C**). High expression protein-coding RNA included matrix metalloproteinase 8 (*MMP8*), resistin (*RETN*) and lipocalin 2 (*LCN2*). Low expression protein-coding RNA included a Na+/Ca2+ exchanger (*SLC8A1*), membrane metalloendopeptidase (*MME*) and interleukin (IL-) 6 receptor (*IL6R*). Long non-coding RNA included lincRNA lung cancer associated transcript 1 (*LUCAT1*; low expression) and antisense RNA (*LRRC75A-AS1*; high expression) (**Figure 2C**). No significant alterations were identified in small non-coding RNA expression profiles. Evaluating RNA expression in patients discordant for survival after 28

days, identified 146 significantly altered protein-coding RNA (**Figure 2 - figure supplement 1C)**. No significant differences were uncovered in non-coding RNA expression profiles, suggesting that non-coding RNA profiles obtained on ICU admission may not be suitable as mortality predictors.

**Protein-coding and non-coding RNA profiles of sepsis patients relative to human endotoxemia.**

Previous studies have compared the protein-coding RNA response in patients with sepsis or trauma (non-septic) to the response after LPS administration to healthy volunteers in a controlled clinical setting (human endotoxemia).[8, 28-33] Here, we sought to extend on those observations by evaluating long and small non-coding RNA expression in sepsis relative to temporal leukocyte responses in human endotoxemia (**Figure 3**). As previously reported in this model,[8, 28-30] robust alterations in protein-coding RNA expression were noted after 2, 4 and 6 hours of LPS administration (**Figure 3 - figure supplement 1**). Fold expression in sepsis (relative to health) was directly correlated to fold expression after 2, 4 and 6 hours LPS (**Figure 3A**). Long non-coding RNA expression was robustly altered in endotoxemia, with 2361, 5053, 2925 and 43 significant differences after 2, 4, 6 and 24 hours endotoxemia, respectively (**Figure 3 - figure supplement 2A**). Pseudogenes, lincRNA and antisense RNA were the most abundant long non-coding RNA biotypes (**Figure 3B**). Small non-coding RNA were modestly altered in human endotoxemia (**Figure 3 - figure supplement 2B**). The most abundant biotypes of small RNA were miRNA (**Figure 3C**). Compared to fold expression in sepsis revealed significant correlations after 2, 4 and 6 hours of endotoxemia (**Figure 3D**). The highest $r^2$ was found for sepsis and 4 hours post-LPS ($r^2 = 0.51$). Correlation analysis of small RNA fold expression during endotoxemia against fold expression in sepsis revealed indirect correlations (**Figure 3E**).

## Functional inference of non-coding RNA

To better understand the functional organization of the non-coding leukocyte transcriptome in sepsis, particularly long non-coding RNA, we undertook a guilt-by-association approach. On the basis of a bi-weight midcorrelation matrix of the most variable protein-coding and long non-coding RNA (n=8539; coefficient of variation > 5%) in sepsis patients only (**Figure 4**), a weighted network was built with scale-free topology (**Figure 4 - figure supplement 1A**).[34-36] Hierarchical clustering uncovered 23 network modules (clusters) each harboring more than 100 inter-correlating RNA transcripts (**Figure 4A** and **Figure 4 - figure supplement 1B**). Of the 8539 RNA transcripts, 158 transcripts did not cluster (designated as a grey module). Seventeen modules were associated to specific gene ontologies or canonical signaling pathways that included cell death/olfactory receptor activity/cell-cycle G2/M DNA damage checkpoint and regulation (turquoise module, n=1001 transcripts) and RNA biosynthesis/RNA binding (yellow module, n=579 transcripts) (**Figure 4A**). Eight modules in the co-expression network were significantly enriched for long non-coding RNA relative to protein-coding RNA (Fisher's adjusted $p < 0.01$; **Figure 4B**). This suggests the leukocyte long non-coding transcriptome of sepsis patients is primarily co-expressed with protein-coding RNA, but 34% of non-coding RNA modules were organized into distinct units. Evaluation of total and intra-module connectivities, which measure the importance of each module relative to the overall structure of co-expression networks,[34] identified two "driver" modules, namely the cell death/olfactory receptor activity/cell-cycle G2/M DNA damage checkpoint and regulation (turquoise module, n=1001 transcripts) and RNA biosynthesis/RNA binding (yellow module, n=579 transcripts) modules (**Figure 4C, D** and **Figure 4 - figure supplement 1C**). The former module included protein-coding RNA encoding ATM serine/threonine kinase (*ATM*), TNF alpha induced protein 3

(*TNFAIP3* or A20), histone deacetylase 2 (*HDAC2*) and mucosa-associated lymphoid tissue lymphoma translocation protein 1 (*MALT1*) paracaspase (**Figure 4D**). Non-coding RNA included *GABPB1-AS1*, *THAP9-AS1* and *SCARNA9*. We subsequently focused our attention on integrating miRNA profiles to the co-expression network. Considering miRNA profiles that were significantly altered in sepsis patients relative to health (**Figure 1C**), and miRNA-to-gene interactions (miRWalk method), we detected 49 small RNAs in 5 network modules with explained variance estimated > 20%, including *hsa-miR-200c-3p* (translation initiation module*)*, *SNORD84 (*regulation of cytokine secretion/Toll-like receptor (TLR) signaling module*)*, *HBII-276* (translation initiation module) and *hsa-miR-1275* (sensory perception of chemical stimulus/olfactory receptor activity module) and *hsa-miR-664b-3p* (neutrophil degranulation/extracellular exosome module) (**Figure 4E**). Of note, *hsa-miR-200c-3p* has been shown to modify TLR4 signaling efficiency dependent on MYD88-mediated pathways in an embryonic kidney cell line (HEK293).[37]

Next, we evaluated the association of network modules to soluble mediators of the host response and clinical severity scores. Neutrophil degranulation (secretory; red), protein ubiquitination (pink) and mitotic cell cycle (tan) modules correlated with soluble mediators of inflammation (C reactive protein (CRP), interleukin (IL)-6, IL-10, IL-8), endothelial responses (E-Selectin and angiopoietin-2 (ANG2)), coagulation (D-Dimer) and clinical variables of disease severity (**Figure 5A**). In contrast, antigen presentation/Th1-Th2 cell activation (green module), regulation of cytokine secretion/TLR signaling (black module) and type-I interferon signaling/double stranded RNA binding (salmon module) were indirectly correlated to various soluble mediators and clinical severity indices. Patients with septic shock showed significantly higher neutrophil degranulation (secretory) expression patterns (**Figure 5B**). Protein-coding RNA transcripts in the neutrophil degranulation (secretory) module included matrix metalloproteinases (*MMP8* and

*MMP9*), neutrophil activation cluster of differentiation 177 (*CD177*), lipocalin 2 (*LCN2*) and arginase 1 (*ARG1*) (**Figure 5C**). LincRNA and antisense RNA included an inducer of differentiation *MYOSLID* (Myocardin-Induced Smooth Muscle LncRNA, Inducer Of Differentiation), cell proliferation and metastasis associated antisense RNA of the titin gene (*TTN-AS1*) and a IL10 receptor beta subunit antisense RNA, *IL10RB-AS1*. Calculating intra-modular connectivities enabled us to define "hub" transcripts, which are understood to represent cogs in the functional output of a network module,[34, 38] and identified *MYOSLID* (neutrophil degranulation; red module) and *LUCAT1* (Lung Cancer Associated Transcript 1) in the TLR-signaling (black) module, as module "hubs". In line with their respective module eigengene correlations to inflammatory response markers, *MYOSLID* expression was directly correlated with levels of inflammatory response markers IL-6, IL-8, IL-10, and acute phase response protein CRP (**Figure 5D**). In contrast, *LUCAT1* expression was indirectly correlated to soluble mediators of inflammation, except for CRP (**Figure 5E**).

## Discussion

In this study we found that the transcriptional changes in critically ill patients with sepsis are not exclusive to protein-coding RNAs. Whole blood long non-coding RNAs, and to a lesser extent small non-coding RNAs, were significantly altered in sepsis patients relative to healthy subjects. The pattern of protein-coding and long non-coding RNA profiles in sepsis were mimicked by expression profiles in a human endotoxemia model, notably at a time point indicative of endotoxin tolerance. Small non-coding RNA profiles in sepsis patients were not recapitulated in human endotoxemia. In general, common clinical characteristics explained low proportions of variation in protein-coding and non-coding RNA profiles, suggesting that variation in leukocyte responses are largely not explained by clinical parameters. Leveraging on the

concepts of network biology, protein-coding and non-coding RNA were clustered as functional biological units with RNA binding/RNA biosynthesis and cell death/olfactory receptor activity/cell-cycle G2-M DNA damage checkpoint and regulation modules central to network architecture.

Advances in genomics, notably massively parallel cDNA sequencing, have shown that active transcription is not exclusive to protein-coding RNA regions.[14] Regions of the genome void of protein-coding genes have since been shown to be actively transcribed in the context of various diseases.[21] Small non-coding RNAs, mainly microRNAs, as well as long non-coding RNAs were linked to specific immune processes.[24, 39] While microRNAs have been established as veritable epigenetic modifiers of transcriptional outputs, studies on the functional aspects of long non-coding RNAs have only recently begun. However, those studies were centered primarily on mouse models.[18, 19] This presents a problem for translation to human physiology because non-coding RNA sequences are typically not conserved between species [40]. Furthermore, expression of non-coding RNAs was shown to exhibit substantially higher inter-individual variation in healthy subjects as compared to protein-coding RNAs alone.[41] In line with those observations our data showed that long non-coding RNA expression patterns were far more variable across individuals (healthy or sepsis) than protein-coding and small non-coding RNAs. The sources of increased inter-individual variation in long non-coding RNA expression relative to protein-coding and small non-coding RNAs are as yet unknown. Lower conservation coupled with faster evolution rates of long non-coding RNA regions, which seemingly harbor more single nucleotide polymorphisms (SNPs) than protein-coding genes,[42] as well as the possibility of their relatively higher susceptibility to environmental and lifestyle factors,[43] may be at the basis of the extensive variation in long non-coding RNA expression.

In line with previous studies,[31, 33] we found that protein-coding RNA alterations during endotoxemia mimicked those that ensue in sepsis patients. The human endotoxemia model is a highly relevant *in vivo* model of acute systemic inflammation in the context of a controlled clinical setting.[44] In general, the model is characterized by a robust systemic response, including leukocyte transcriptional responses, exhibiting shared and unique temporal changes that resolve within 24 hours of bolus administration.[28, 30] In extension to the previously reported data, based on a single time-point of human endotoxemia,[31, 33] we found that the correlation between sepsis and human endotoxemia was also dependent, at least in part, on timing of the response to LPS. The highest correlation was found at 4 hours, a time point at which the capacity of cytokine production by leukocytes is typically reduced in the human endotoxemia model, indicative of endotoxin tolerance.[8, 45] Long non-coding RNA alterations in human endotoxemia also mimicked those in sepsis, with similar time dependencies as protein-coding RNA. In contrast, small non-coding RNA expression profiles in sepsis patients were not reliably recapitulated in human endotoxemia, primarily showing indirect correlations. This may be due to typically low expression patterns of miRNA, compared to protein-coding and long non-coding RNA, and reported high specificities of miRNA to developmental stage and cell-type.[46] The host response during infection is characterized by a balance between resistance (seeking to limit the pathogen load) and tolerance (aiming to retain cell and organ functions).[47] In sepsis both mechanisms can become uncontrolled, wherein aberrant activation of resistance pathways results in tissue damage and inadequate tolerance can cause immune suppression with enhanced susceptibility to secondary infections.[48] While our time-sequential data in healthy humans injected with LPS suggest that coding and long non-coding RNA profiles in blood leukocytes of sepsis patients particularly reflect a tolerant state, time course studies in patients are needed to

increase the insight into the role of distinct RNA species in the interplay between resistance and tolerance.

A substantial proportion of variance in protein-coding and non-coding RNA expression in critically ill patients with sepsis remained unexplained. Other sources of variation, not assessed in this study, include patient genetics and time between the onset of sepsis and ICU admission.[49, 50] The former represents an important source of inter-individual variation where SNPs segregating in populations are in part tightly related to RNA expression variability.[49] This was shown in a recent prospective study in sepsis due to community-acquired pneumonia (CAP), wherein SNPs influencing gene expression patterns were identified.[10] The time of onset of sepsis is a current “black box” in the field as it cannot be accurately determined, thereby resulting in considerable uncertainty since patients are presumably admitted to the ICU at various stages of the sepsis syndrome. Despite overall low percent variation explained specific protein-coding and long non-coding RNA transcripts had high percent variation attributable to, particularly, primary diagnosis that included infections site (lung or abdomen) and place of acquisition (community or hospital), which may constitute important proxies to discern organ-specific infections that are typically caused by different causal pathogens.[51-53]

Determining cellular biological pathways wherein long non-coding RNA function is a major challenge. To address this challenge, we undertook a guilt-by-association strategy that sought to position long non-coding RNA in co-expression modules of tightly correlating protein-coding RNA, thereby infer on functional outputs of long non-coding RNA by virtue of the pathways that associate with protein-coding RNA in each module. By leveraging on the concepts of scale free networks,[54] we built a map of protein-coding and non-coding RNA relationships that pointed to cell death/olfactory receptor activity/cell-cycle G2/M DNA damage checkpoint and regulation (turquoise module) and RNA biosynthesis/RNA binding (yellow module) as

central to the organization of the co-expression network. Cell death or exhaustion, particularly in lymphocytes, have been proposed as causal features of immunosuppression and lethality in sepsis.[55] Our findings further strengthen this hypothesis and position previously unknown non-coding RNA, including an autophagy and chemical stress responder *GABPB1-AS1*,[56, 57] as putative regulators of cell death in the context of sepsis. Interestingly, protein-coding RNA in the cell death (turquoise) module also included olfactory receptors and cell-cycle DNA damage regulators. Modulation of DNA damage responses was demonstrated as a potential therapeutic path that might be exploited to confer protection to severe sepsis.[58] Little is known about olfactory receptors in non-chemosensory cells, but a growing body of evidence suggests they are not exclusive to the nose.[59] They have been shown to be involved in cell-cell recognition, migration, proliferation and apoptosis.[60]

In conclusion, we here describe the non-coding RNA landscape in blood leukocytes of sepsis patients upon admission to the ICU. By considering non-coding RNA expression patterns in relation to protein-coding RNA we provide an important layer to the blood leukocyte "regulome" in a clinical context, which may facilitate prioritization of non-coding RNA in future functional studies.

## Materials and Methods

| **Key Resources Table** | | | | |
|---|---|---|---|---|
| **Reagent type (species) or resource** | **Designation** | **Source or reference** | **Identifiers** | **Additional information** |

| | | | | |
|---|---|---|---|---|
| biological sample (Homo sapiens) | Total RNA | Leukocytes | | |
| commercial assay or kit | PAXgene Blood miRNA kit | Qiagen | Cat no./ID: 763134 | |
| commercial assay or kit | Human Transcriptome Array 2.0 | Affymetrix; Thermo Fisher | | microarray |
| commercial assay or kit | miRNA 4.1 96-array plate | Affymetrix; Thermo Fisher | | microarray |
| commercial assay or kit | FlexSet cytometric bead arrays | BD Biosciences | | |
| commercial assay or kit | Immunoturbidimetric assay | Roche diagnostics | | |
| commercial assay or kit | Luminex Flow Cytometry Analyzer | Luminex Corp. | RRID:SCR_018025 | |
| commercial assay or kit | Sysmex CA-1500 System | Siemens Healthineers | | |
| chemical compound, drug | Lipopolysaccharide-Escherichia coli, 100 ng/ml, Ultrapure | Invivogen | Cat#0111:B4 | |
| software, algorithm | R Project for Statistical Computing, (version 3.5.0) | R Development Core Team | RRID:SCR_001905 | |
| software, algorithm | Oligo (version 1.44) | Bioconductor | Carvalho BS & Irizarry RA Bioinformatics 2010, 26:2363-2367. RRID:SCR_015729 | |
| software, algorithm | SVA (version 3.28) | Bioconductor | Leek JT & Storey JD Plos Genetics 2007, 3:1724-1735. | |

| | | | | |
|---|---|---|---|---|
| | | | RRID:SCR_012836 | |
| software, algorithm | genefilter (version 1.62) | Bioconductor | Bourgon R et.al. PNAS 2010, 107:9546-9551. | |
| software, algorithm | arrayQualityMetrics | Bioconductor | Kauffmann A, et.al. Bioinformatics 2009, 25:415-416. RRID:SCR_001335 | |
| software, algorithm | Affymetrix Transcriptome Analysis Console | Affymetrix | RRID:SCR_018718 | |
| software, algorithm | limma (version 3.36) | Bioconductor | Smyth GK. Springer; 2005: 397-420. RRID:SCR_010943 | |
| software, algorithm | Ingenuity pathway analysis software | Qiagen | RRID:SCR_008653 | |
| software, algorithm | WGCNA (version 1.64) | Bioconductor | Langfelder P & Horvath S. BMC Bioinformatics 2008, 9:559. RRID:SCR_003302 | |
| software, algorithm | miR-Walk 2.0 | University of Heidelberg, Germany | Dweep H, et.al. J Biomed Inform 2011, 44:839-847. | |
| software, algorithm | variancePartition (version 1.10) | Bioconductor | Hoffman GE & Schadt EE BMC Bioinformatics 2016, 17:483. | |
| software, algorithm | mixOmics | Bioconductor | Rohart F, et.al. PLoS Comput Biol 2017, 13:e1005752. RRID:SCR_016889 | |
| other | Deposited data super-series | Gene Expression Omnibus | GSE134364 | |

**Patient population and inclusion criteria**

This study was part of the Molecular Diagnosis and Risk Stratification of sepsis (MARS) project, a prospective observational study in the mixed ICUs of two tertiary teaching hospitals in the Netherlands (Academic Medical Center, Amsterdam and University Medical Center Utrecht, Utrecht) (ClinicalTrials.gov identifier NCT01905033).[51, 61, 62] For the current study, we selected consecutive patients with sepsis from the MARS biorepository who were older than 18 years of age, had been admitted to the ICU between July 2012 and January 2014. Sepsis (n=156) was defined as the presence of community-acquired pneumonia (CAP), hospital-acquired pneumonia (HAP) or intra-abdominal infection diagnosed within 24 hours of ICU admission with a culture proven or probable likelihood using criteria as described[63], accompanied by at least one additional general, inflammatory, hemodynamic, organ dysfunction, or tissue perfusion variable described in the third international consensus definitions for sepsis and septic shock.[64] Patients with aspiration pneumonia, with multiple sites of infection, and patients admitted to the ICU more than 2 days after the initiation of antibiotics were excluded. All readmissions and patients transferred from another ICU were also excluded, except when patients were referred to one of the study centers on the same day of presentation to the first ICU. Severity was assessed by APACHE IV[63] and SOFA score excluding the central nervous system component.[65] Shock was qualified by the use of vasopressors (norepinephrine, epinephrine or dopamine) for hypotension in a norepinephrine-equivalent dose of more than 0.1 µg/kg/min in patients with a SOFA score of at least 2.[64] Blood was collected in PAXgene tubes (Becton-Dickinson, Breda, The Netherlands) and ethylenediaminetetraacetic acid (EDTA) vacutainer tubes within 24 hours of ICU admission. Definitions of comorbid and immunocompromised conditions are reported in the online data supplement.

**Healthy participants and endotoxemia**

PAXgene and EDTA tubes were also obtained from 82 healthy subjects. Eight male subjects were exposed to intravenous LPS in a Phase I, randomized, single-blind, parallel group, placebo controlled study (clinicaltrials.gov identifier NCT02328612); the subjects who received placebo were used in the current study.[30] Subjects were infused with LPS over one minute (2 ng/kg; from *Escherichia* [*E.*] *coli*, US standard reference endotoxin, kindly provided by Anthony Suffredini, National Institute of Health, Bethesda, MD). Whole blood was collected in PaxGene Blood tubes (Qiagen) before and 2, 4, 6, 24 hours after LPS administration.

**Immunological markers**

EDTA-anticoagulated blood plasma collected on ICU admission was used for soluble mediator measurements. Interleukin (IL)-6, IL-8, IL-10, soluble intercellular adhesion molecule-1 (ICAM-1), soluble E-selectin and fractalkine were measured using FlexSet cytometric bead arrays (BD Biosciences, San Jose, CA) using a FACS Calibur (Becton Dickinson, Franklin Lakes, NJ, NJ, USA). Neutrophil gelatinase-associated lipocalin (NGAL), Angiopoietin-1, angiopoietin-2, protein C, antithrombin, matrix metalloproteinase (MMP)-8 (R&D Systems, Abingdon, UK), and D-dimer (Procartaplex, eBioscience, San Diego, CA) were measured by Luminex multiplex assay using a BioPlex 200 (BioRas, Hercules, CA). C-reactive protein (CRP) was determined by an immunoturbidimetric assay (Roche diagnostics). Platelet counts were determined by hemocytometry, prothrombin time (PT) and activated partial thromboplastin time (aPTT) by using a photometric method with Dade Innovin Reagent or by Dade Actin FS Activated PTT Reagent, respectively (Siemens Healthcare Diagnostics). Normal biomarker values were obtained from 27 age- and sex-matched healthy subjects, except for CRP, platelet counts, PT and aPTT (routine laboratory reference values).

## Microarrays and data processing

Total RNA was isolated by means of PaxGene blood miRNA isolation kit (Thermo-Fisher) as per manufacturer's instructions. Quality RNA (Agilent 2100 Bioanalyzer, Agilent Technologies; RIN > 6) was processed and hybridized to either the GeneChip Human Transcriptome Array (HTA) 2.0 (Thermo-Fisher) or the miRNA 4.1 96-array plate (Thermo-Fisher) following manufacturer's instructions. Both arrays were done on all samples (sepsis patients, controls and healthy subjects injected with LPS). Microarrays were scanned at the Cologne Center for Genomics, Cologne, Germany.

The HTA 2.0 scans (.CEL) were processed in the R language and environment for statistical computing version 3.5.0 (R Development Core Team, Foundation for Statistical Computing, Vienna, Austria). Following robust multi-average (RMA) background-correction, quantile normalization and $\log_2$-transformation using the oligo method (version 1.44),[66] data were evaluated for non-experimental chip effects by means of surrogate variable analysis (SVA; version 3.28) and adjusted using the combat method.[67] Probes were annotated using biomart (version 2.36.1),[68] and low expression probes were filtered by means of the genefilter method (version 1.62).[69] The miRNA-4.1 scans (.CEL) were analyzed by means of Affymetrix Expression Console software (Thermo-Fisher). Probes were normalized using the RMA method and detection above background (DABG) probe level detection. Homo sapiens annotated probes with detection p-value $< 0.05$ in at least one sample were considered for downstream analyses. Quality of HTA2.0 and miRNA-4.1 arrays was evaluated by means of the arrayqualitymetrics R package.[70] Comparisons between study groups were done using the limma method (version 3.36)[71] and significance was demarcated by Benjamini-Hochberg multiple test adjusted probabilities (adjusted $p < 0.01$). The linear model included age and sex as additive covariates.

The molecular-distance-to-health (MDTH) index was calculated as described previously.[25, 26] Ingenuity Pathway Analysis (Ingenuity systems, Qiagen) was used to determine the most significant canonical signaling pathways for elevated and reduced protein-coding RNA transcripts considering adjusted Fisher's probabilities (adjusted $p < 0.05$) specifying the Ingenuity knowledgebase as reference and human species. All other parameters were default.

The novelty of our study, that is, profiling non-coding RNA expression in leukocytes of patients with sepsis, precludes an adequate study power estimation. However, considering known co-regulation with protein-coding RNA expression, we provide study power estimates based on previous observations in typical gene expression studies.[8-10] Considering a false discovery rate of 5%, beta error level 5% (95% power), and typical effect sizes greater than 0.25 in sepsis relative to health, a sample size of 42 per group was estimated. In addition, 8 healthy volunteers in a human endotoxemia challenge would have more than 95% power to detect differences relative to pre-challenge (baseline) samples.[8, 10, 28-33] Using a continuous model, we estimated 156 patients would have more than 98% power to detect significant associations with demographic or clinical variables (false-discovery rates of 5%).

**Co-expression network and pathway analysis**

The weighted gene co-expression network analysis (WGCNA) method (version 1.64) was used to build the leukocyte co-expression network as described previously.[34, 36, 38] A pair-wise biweight midcorrelation matrix of the most variable transcripts (coefficient of variation > 5%) was transformed into an adjacency matrix by using a "soft" power function of 8 ensuring scale-free topology.[34, 38] The adjacency matrix was further transformed into a topological overlap matrix to enable the identification of modules (clusters) encompassing highly inter-correlating RNA transcripts by using a dynamic tree cut method (version 1.63).[34, 38] Modules were

summarized by means of the eigengene value, defined as the first principal component of the module expression matrix and the module membership measure. Protein-coding RNA in each module were analyzed for enrichment of gene ontologies for biological processes (GO:BP), molecular function (GO:MF) and cellular compartment (GO:CC) using the Gene Ontology Consortium database with significance defined by adjusted p-value < 0.05 (www.geneontology.org).[72] Biofunctions were predicted using Ingenuity Pathways software (Ingenuity pathway analysis, Qiagen Bioinformatics) specifying activation z-score < 2 or > 2 and adjusted p-value < 0.05. The miR-Walk atlas of gene-miRNA-target interactions was used to evaluate predicted interactions of miRNA with module-specific genes by specifying the miR-Walk algorithm.[73, 74] Human species annotations and 3' untranslated region (UTR) interactions as well as a minimum seed length equating to 7 were specified. All other parameters were default.

**Statistics**

Statistical analysis was performed in the R statistical environment (v 3.5.0). Comparison of continuous data between categories was done with the Wilcoxon rank sum test. Correlation analysis of continuous data was performed using Pearson's method unless otherwise stated as well as the coefficient of determination ($r^2$). Categorical data were analyzed by Fisher exact tests or Chi-squared tests. Multiple comparison (Benjamini-Hochberg) adjusted p-values < 0.05 defined significance. The proportion of variance in RNA expression explained by demographics and clinical characteristics was calculated using a multivariate approach implemented in the variancePartition method (version 1.10).[27] A multivariate linear model was fit including age, gender, primary diagnosis, total SOFA, APACHE IV scores, shock and Charlson comorbidity indices. Principal component analysis was done using the mixOmics package, specifying 10

components.[75] Data is presented in the form of volcano plots, pie charts, dot plots, bar charts, circular and violin plots.

## Declarations

### Ethics approval and consent to participate

The institutional review boards of both participating centers approved an opt-out consent method (IRB No. 10-056C). The Dutch Central Committee on Research Involving Human Subjects and the Medical Ethics Committee of the Academic Medical Center, Amsterdam, the Netherlands, approved the study. Written informed consent was obtained from all healthy participants.

### Availability of data and materials

The datasets generated and analysed during the current study are available in the Gene Expression Omnibus of the National Center for Biotechnology Information repository with primary data accession numbers GSE134364 (super-series), GSE134347 for patients and healthy volunteers (HTA 2.0 microarray), GSE134356 for the human endotoxemia model samples (HTA 2.0 microarray) and GSE134358 for all patients, healthy volunteers and human endotoxemia samples (miRNA-4.1 microarray).

### Competing interests

The authors declare that they have no competing interests.

### Funding

This study was funded by the Center for Translational Molecular Medicine (www.ctmm.nl; grant 04I-201). In addition, the research leading to the results reported was conducted as part of the

COMBACTE consortium (www.COMBACTE.com). COMBACTE receives support from the Innovative Medicines Initiative Joint Undertaking under grant agreement n° 115523 | 115620 | 115737 resources of which are composed of financial contribution from the European Union Seventh Framework Programme (FP7/2007-2013) and EFPIA companies in kind contribution.

## Acknowledgements

The authors thank all patients and healthy volunteers who participated in this study, as well as the critical care nursing staff at both the AMC and UMCU ICUs. Members of the MARS consortium were: from Amsterdam University Medical Centers, location Academic Medical Center, University of Amsterdam, the Netherlands: Friso M. de Beer, Lieuwe D. J. Bos, Gerie J. Glas, Roosmarijn T. M. van Hooijdonk, Janneke Horn, Mischa A. Huson, Laura R. A. Schouten, Marleen Straat, Luuk Wieske, Maryse A. Wiewel, Esther Witteveen; from University Medical Center Utrecht, Utrecht, the Netherlands: David S.Y. Ong, Jos F. Frencken, Maria E. Koster-Brouwer, Kirsten van de Groep, Diana M. Verboom.

## References

1. Angus DC, van der Poll T: **Severe Sepsis and Septic Shock.** *New England Journal of Medicine* 2013, **369:**840-851.
2. Cecconi M, Evans L, Levy M, Rhodes A: **Sepsis and septic shock.** *Lancet* 2018, **392:**75-87.
3. Fleischmann C, Scherag A, Adhikari NK, Hartog CS, Tsaganos T, Schlattmann P, Angus DC, Reinhart K, International Forum of Acute Care T: **Assessment of Global Incidence and Mortality of Hospital-treated Sepsis. Current Estimates and Limitations.** *Am J Respir Crit Care Med* 2016, **193:**259-272.
4. Organization WH: **Resolution WHA70.7: Improving the prevention, diagnosis and clinical management of sepsis.** 2017.
5. Marshall JC: **Why have clinical trials in sepsis failed?** *Trends Mol Med* 2014, **20:**195-203.
6. Tse MT: **Trial watch: Sepsis study failure highlights need for trial design rethink.** *Nat Rev Drug Discov* 2013, **12:**334.
7. van der Poll T, van de Veerdonk FL, Scicluna BP, Netea MG: **The immunopathology of sepsis and potential therapeutic targets.** *Nat Rev Immunol* 2017, **17:**407-420.

471 8. Cheng SC, Scicluna BP, Arts RJ, Gresnigt MS, Lachmandas E, Giamarellos-Bourboulis EJ, Kox M,
472 Manjeri GR, Wagenaars JA, Cremer OL, et al: **Broad defects in the energy metabolism of**
473 **leukocytes underlie immunoparalysis in sepsis.** *Nat Immunol* 2016, **17:**406-413.
474 9. Scicluna BP, van Vught LA, Zwinderman AH, Wiewel MA, Davenport EE, Burnham KL, Nurnberg P,
475 Schultz MJ, Horn J, Cremer OL, et al: **Classification of patients with sepsis according to blood**
476 **genomic endotype: a prospective cohort study.** *Lancet Respir Med* 2017, **5:**816-826.
477 10. Davenport EE, Burnham KL, Radhakrishnan J, Humburg P, Hutton P, Mills TC, Rautanen A, Gordon
478 AC, Garrard C, Hill AV, et al: **Genomic landscape of the individual host response and outcomes**
479 **in sepsis: a prospective cohort study.** *Lancet Respir Med* 2016, **4:**259-271.
480 11. Wong HR, Cvijanovich N, Lin R, Allen GL, Thomas NJ, Willson DF, Freishtat RJ, Anas N, Meyer K,
481 Checchia PA, et al: **Identification of pediatric septic shock subclasses based on genome-wide**
482 **expression profiling.** *BMC Med* 2009, **7:**34.
483 12. Liu G, Mattick JS, Taft RJ: **A meta-analysis of the genomic and transcriptomic composition of**
484 **complex life.** *Cell Cycle* 2013, **12:**2061-2072.
485 13. Kapranov P, Cawley SE, Drenkow J, Bekiranov S, Strausberg RL, Fodor SP, Gingeras TR: **Large-**
486 **scale transcriptional activity in chromosomes 21 and 22.** *Science* 2002, **296:**916-919.
487 14. Carninci P, Kasukawa T, Katayama S, Gough J, Frith MC, Maeda N, Oyama R, Ravasi T, Lenhard B,
488 Wells C, et al: **The transcriptional landscape of the mammalian genome.** *Science* 2005,
489 **309:**1559-1563.
490 15. Ponjavic J, Ponting CP, Lunter G: **Functionality or transcriptional noise? Evidence for selection**
491 **within long noncoding RNAs.** *Genome Res* 2007, **17:**556-565.
492 16. Zhu S, Li W, Liu J, Chen CH, Liao Q, Xu P, Xu H, Xiao T, Cao Z, Peng J, et al: **Genome-scale deletion**
493 **screening of human long non-coding RNAs using a paired-guide RNA CRISPR-Cas9 library.** *Nat*
494 *Biotechnol* 2016, **34:**1279-1286.
495 17. Gebert LFR, MacRae IJ: **Regulation of microRNA function in animals.** *Nat Rev Mol Cell Biol* 2018.
496 18. Atianand MK, Hu W, Satpathy AT, Shen Y, Ricci EP, Alvarez-Dominguez JR, Bhatta A, Schattgen
497 SA, McGowan JD, Blin J, et al: **A Long Noncoding RNA lincRNA-EPS Acts as a Transcriptional**
498 **Brake to Restrain Inflammation.** *Cell* 2016, **165:**1672-1685.
499 19. Carpenter S, Aiello D, Atianand MK, Ricci EP, Gandhi P, Hall LL, Byron M, Monks B, Henry-Bezy M,
500 Lawrence JB, et al: **A long noncoding RNA mediates both activation and repression of immune**
501 **response genes.** *Science* 2013, **341:**789-792.
502 20. Bao Z, Yang Z, Huang Z, Zhou Y, Cui Q, Dong D: **LncRNADisease 2.0: an updated database of long**
503 **non-coding RNA-associated diseases.** *Nucleic Acids Res* 2019, **47:**D1034-D1037.
504 21. Esteller M: **Non-coding RNAs in human disease.** *Nat Rev Genet* 2011, **12:**861-874.
505 22. Carpenter S, Fitzgerald KA: **Cytokines and Long Noncoding RNAs.** *Cold Spring Harb Perspect Biol*
506 2018, **10**.
507 23. Atianand MK, Fitzgerald KA: **Long non-coding RNAs and control of gene expression in the**
508 **immune system.** *Trends Mol Med* 2014, **20:**623-631.
509 24. Mehta A, Baltimore D: **MicroRNAs as regulatory elements in immune system logic.** *Nat Rev*
510 *Immunol* 2016, **16:**279-294.
511 25. Berry MPR, Graham CM, Mcnab FW, Xu ZH, Bloch SAA, Oni T, Wilkinson KA, Banchereau R,
512 Skinner J, Wilkinson RJ, et al: **An interferon-inducible neutrophil-driven blood transcriptional**
513 **signature in human tuberculosis.** *Nature* 2010, **466:**973-U998.
514 26. Dunning J, Blankley S, Hoang LT, Cox M, Graham CM, James PL, Bloom CI, Chaussabel D,
515 Banchereau J, Brett SJ, et al: **Progression of whole-blood transcriptional signatures from**
516 **interferon-induced to neutrophil-associated patterns in severe influenza.** *Nat Immunol* 2018,
517 **19:**625-635.

518 27. Hoffman GE, Schadt EE: **variancePartition: interpreting drivers of variation in complex gene**
519 **expression studies.** *BMC Bioinformatics* 2016, **17:**483.
520 28. Calvano SE, Xiao WZ, Richards DR, Felciano RM, Baker HV, Cho RJ, Chen RO, Brownstein BH, Cobb
521 JP, Tschoeke SK, et al: **A network-based analysis of systemic inflammation in humans.** *Nature*
522 2005, **437:**1032-1037.
523 29. Scicluna BP, van 't Veer C, Nieuwdorp M, Felsmann K, Wlotzka B, Stroes ES, van der Poll T: **Role**
524 **of tumor necrosis factor-a in the human systemic endotoxin-induced transcriptome.** *PLoS One*
525 2013**:**e79051.
526 30. Perlee D, van Vught LA, Scicluna BP, Maag A, Lutter R, Kemper EM, van 't Veer C, Punchard MA,
527 Gonzalez J, Richard MP, et al: **Intravenous Infusion of Human Adipose Mesenchymal Stem Cells**
528 **Modifies the Host Response to Lipopolysaccharide in Humans: A Randomized, Single-Blind,**
529 **Parallel Group, Placebo Controlled Trial.** *Stem Cells* 2018, **36:**1778-1788.
530 31. Seok J, Warren H, Cuenca AG, Mindrinos MN, Baker HV, Xu W, Richards DR, McDonald-Smith GP,
531 Gao H, Hennessy L, et al: **Genomic responses in mouse models poorly mimic human**
532 **inflammatory diseases.** *Proceedings of the National Academy of Sciences of the United States of*
533 *America* 2013, **110:**3507-3512.
534 32. Xiao W, Mindrinos MN, Seok J, Cuschieri J, Cuenca AG, Gao H, Hayden DL, Hennessy L, Moore EE,
535 Minei JP, et al: **A genomic storm in critically injured humans.** *Journal of Experimental Medicine*
536 2011, **208:**2581-2590.
537 33. Takao K, Miyakawa T: **Genomic responses in mouse models greatly mimic human inflammatory**
538 **diseases.** *Proc Natl Acad Sci U S A* 2015, **112:**1167-1172.
539 34. Langfelder P, Horvath S: **WGCNA: an R package for weighted correlation network analysis.** *BMC*
540 *Bioinformatics* 2008, **9:**559.
541 35. Langfelder P, Horvath S: **Fast R Functions for Robust Correlations and Hierarchical Clustering.** *J*
542 *Stat Softw* 2012, **46**.
543 36. Scicluna BP, van Lieshout MH, Blok DC, Florquin S, van der Poll T: **Modular Transcriptional**
544 **Networks of the Host Pulmonary Response during Early and Late Pneumococcal Pneumonia.**
545 *Mol Med* 2015, **21:**430-441.
546 37. Wendlandt EB, Graff JW, Gioannini TL, McCaffrey AP, Wilson ME: **The role of microRNAs miR-**
547 **200b and miR-200c in TLR4 signaling and NF-kappaB activation.** *Innate Immun* 2012, **18:**846-
548 855.
549 38. Zhao W, Langfelder P, Fuller T, Dong J, Li A, Hovarth S: **Weighted gene coexpression network**
550 **analysis: state of the art.** *J Biopharm Stat* 2010, **20:**281-300.
551 39. Fitzgerald KA, Caffrey DR: **Long noncoding RNAs in innate and adaptive immunity.** *Curr Opin*
552 *Immunol* 2014, **26:**140-146.
553 40. Diederichs S: **The four dimensions of noncoding RNA conservation.** *Trends Genet* 2014, **30:**121-
554 123.
555 41. Kornienko AE, Dotter CP, Guenzl PM, Gisslinger H, Gisslinger B, Cleary C, Kralovics R, Pauler FM,
556 Barlow DP: **Long non-coding RNAs display higher natural expression variation than protein-**
557 **coding genes in healthy humans.** *Genome Biol* 2016, **17:**14.
558 42. Necsulea A, Kaessmann H: **Evolutionary dynamics of coding and non-coding transcriptomes.**
559 *Nat Rev Genet* 2014, **15:**734-748.
560 43. Dumeaux V, Olsen KS, Nuel G, Paulssen RH, Borresen-Dale AL, Lund E: **Deciphering normal blood**
561 **gene expression variation--The NOWAC postgenome study.** *PLoS Genet* 2010, **6:**e1000873.
562 44. Lowry SF: **Human endotoxemia: a model for mechanistic insight and therapeutic targeting.**
563 *Shock* 2005, **24 Suppl 1:**94-100.

564 45. de Vos AF, Pater JM, van den Pangaart PS, de Kruif MD, van 't Veer C, van der Poll T: **In vivo**
565 **lipopolysaccharide exposure of human blood leukocytes induces cross-tolerance to multiple**
566 **TLR ligands.** *J Immunol* 2009, **183:**533-542.
567 46. Bernstein E, Kim SY, Carmell MA, Murchison EP, Alcorn H, Li MZ, Mills AA, Elledge SJ, Anderson
568 KV, Hannon GJ: **Dicer is essential for mouse development.** *Nat Genet* 2003, **35:**215-217.
569 47. Schneider DS, Ayres JS: **Two ways to survive infection: what resistance and tolerance can teach**
570 **us about treating infectious diseases.** *Nat Rev Immunol* 2008, **8:**889-895.
571 48. Bauer M, Wetzker R: **The cellular basis of organ failure in sepsis-signaling during damage and**
572 **repair processes.** *Med Klin Intensivmed Notfmed* 2020, **115:**4-9.
573 49. Schadt EE, Monks SA, Drake TA, Lusis AJ, Che N, Colinayo V, Ruff TG, Milligan SB, Lamb JR, Cavet
574 G, et al: **Genetics of gene expression surveyed in maize, mouse and man.** *Nature* 2003,
575 **422:**297-302.
576 50. Maslove DM, Wong HR: **Gene expression profiling in sepsis: timing, tissue, and translational**
577 **considerations.** *Trends Mol Med* 2014, **20:**204-213.
578 51. van Vught LA, Klein Klouwenberg PM, Spitoni C, Scicluna BP, Wiewel MA, Horn J, Schultz MJ,
579 Nurnberg P, Bonten MJ, Cremer OL, et al: **Incidence, Risk Factors, and Attributable Mortality of**
580 **Secondary Infections in the Intensive Care Unit After Admission for Sepsis.** *JAMA* 2016,
581 **315:**1469-1479.
582 52. van Vught LA, Scicluna BP, Wiewel MA, Hoogendijk AJ, Klein Klouwenberg PM, Franitza M, Toliat
583 MR, Nurnberg P, Cremer OL, Horn J, et al: **Comparative Analysis of the Host Response to**
584 **Community-acquired and Hospital-acquired Pneumonia in Critically Ill Patients.** *Am J Respir Crit*
585 *Care Med* 2016.
586 53. Sartelli M: **A focus on intra-abdominal infections.** *World J Emerg Surg* 2010, **5:**9.
587 54. Barabasi AL: **Scale-free networks: a decade and beyond.** *Science* 2009, **325:**412-413.
588 55. Hotchkiss RS, Monneret G, Payen D: **Immunosuppression in sepsis: a novel understanding of**
589 **the disorder and a new therapeutic approach.** *Lancet Infect Dis* 2013, **13:**260-268.
590 56. Tani H, Onuma Y, Ito Y, Torimura M: **Long non-coding RNAs as surrogate indicators for chemical**
591 **stress responses in human-induced pluripotent stem cells.** *PLoS One* 2014, **9:**e106282.
592 57. Luan F, Chen W, Chen M, Yan J, Chen H, Yu H, Liu T, Mo L: **An autophagy-related long non-**
593 **coding RNA signature for glioma.** *FEBS Open Bio* 2019, **9:**653-667.
594 58. Figueiredo N, Chora A, Raquel H, Pejanovic N, Pereira P, Hartleben B, Neves-Costa A, Moita C,
595 Pedroso D, Pinto A, et al: **Anthracyclines induce DNA damage response-mediated protection**
596 **against severe sepsis.** *Immunity* 2013, **39:**874-884.
597 59. Kang N, Koo J: **Olfactory receptors in non-chemosensory tissues.** *BMB Rep* 2012, **45:**612-622.
598 60. Massberg D, Hatt H: **Human Olfactory Receptors: Novel Cellular Functions Outside of the Nose.**
599 *Physiol Rev* 2018, **98:**1739-1763.
600 61. Klein Klouwenberg PM, Ong DSY, Bos LDJ, de Beer FM, van Hooijdonk RTM, Huson MA, Straat M,
601 van Vught LA, Wieske L, Horn J, et al: **Interobserver Agreement of Centers for Disease Control**
602 **and Prevention Criteria for Classifying Infections in Critically Ill Patients.** *Critical Care Medicine*
603 2013, **41:**2373-2378.
604 62. Scicluna BP, Klein Klouwenberg PM, van Vught LA, Wiewel MA, Ong DS, Zwinderman AH, Franitza
605 M, Toliat MR, Nurnberg P, Hoogendijk AJ, et al: **A molecular biomarker to diagnose community-**
606 **acquired pneumonia on intensive care unit admission.** *Am J Respir Crit Care Med* 2015,
607 **192:**826-835.
608 63. Zimmerman JE, Kramer AA, McNair DS, Malila FM: **Acute Physiology and Chronic Health**
609 **Evaluation (APACHE) IV: hospital mortality assessment for today's critically ill patients.** *Crit*
610 *Care Med* 2006, **34:**1297-1310.

611 64. Singer M, Deutschman CS, Seymour CW, Shankar-Hari M, Annane D, Bauer M, Bellomo R,
612 Bernard GR, Chiche JD, Coopersmith CM, et al: **The Third International Consensus Definitions**
613 **for Sepsis and Septic Shock (Sepsis-3).** *JAMA* 2016, **315:**801-810.
614 65. Vincent JL, Moreno R, Takala J, Willatts S, DeMendonca A, Bruining H, Reinhart CK, Suter PM,
615 Thijs LG: **The SOFA (sepsis-related organ failure assessment) score to describe organ**
616 **dysfunction/failure.** *Intensive Care Medicine* 1996, **22:**707-710.
617 66. Carvalho BS, Irizarry RA: **A framework for oligonucleotide microarray preprocessing.**
618 *Bioinformatics* 2010, **26:**2363-2367.
619 67. Leek JT, Storey JD: **Capturing heterogeneity in gene expression studies by surrogate variable**
620 **analysis.** *Plos Genetics* 2007, **3:**1724-1735.
621 68. Smedley D, Haider S, Durinck S, Pandini L, Provero P, Allen J, Arnaiz O, Awedh MH, Baldock R,
622 Barbiera G, et al: **The BioMart community portal: an innovative alternative to large, centralized**
623 **data repositories.** *Nucleic Acids Res* 2015, **43:**W589-598.
624 69. Bourgon R, Gentleman R, Huber W: **Independent filtering increases detection power for high-**
625 **throughput experiments.** *Proc Natl Acad Sci U S A* 2010, **107:**9546-9551.
626 70. Kauffmann A, Gentleman R, Huber W: **arrayQualityMetrics--a bioconductor package for quality**
627 **assessment of microarray data.** *Bioinformatics* 2009, **25:**415-416.
628 71. Smyth GK: **Limma: linear models for microarray data.** In *Bioinformatics and Computational*
629 *Biology Solutions using R.* Edited by R G, VJ C, H W, RA I, S D: Springer; 2005: 397-420
630 72. Ashburner M, Ball CA, Blake JA, Botstein D, Butler H, Cherry JM, Davis AP, Dolinski K, Dwight SS,
631 Eppig JT, et al: **Gene ontology: tool for the unification of biology. The Gene Ontology**
632 **Consortium.** *Nat Genet* 2000, **25:**25-29.
633 73. Dweep H, Sticht C, Pandey P, Gretz N: **miRWalk--database: prediction of possible miRNA**
634 **binding sites by "walking" the genes of three genomes.** *J Biomed Inform* 2011, **44:**839-847.
635 74. Mills JD, Iyer AM, van Scheppingen J, Bongaarts A, Anink JJ, Janssen B, Zimmer TS, Spliet WG, van
636 Rijen PC, Jansen FE, et al: **Coding and small non-coding transcriptional landscape of tuberous**
637 **sclerosis complex cortical tubers: implications for pathophysiology and treatment.** *Sci Rep*
638 2017, **7:**8089.
639 75. Rohart F, Gautier B, Singh A, Le Cao KA: **mixOmics: An R package for 'omics feature selection**
640 **and multiple data integration.** *PLoS Comput Biol* 2017, **13:**e1005752.

641
642

**Table 1. Baseline characteristics and outcomes of critically ill patients with sepsis.**

| Parameter | Sepsis patients (n = 156) |
|---|---|
| Age, years | 62 [50 - 70] |
| Male sex | 98 (62.8) |
| White ethnicity | 140 (89.7) |
| Medical admission | 117 (75.0) |
| Immune suppression | 45 (28.8) |
| Cardiovascular insufficiency | 43 (27.6) |
| Malignancy | 45 (28.8) |
| Renal insufficiency | 18 (11.5) |
| Respiratory insufficiency | 37 (23.7) |
| Charlson comorbidity index | 4 [2 - 6] |
| APACHE IV score | 72 [58 - 92] |
| SOFA score | 7 [4 - 9] |
| Shock | 86 (55.1) |
| Mechanical ventilation | 128 (82.1) |
| *Primary diagnosis* | |
| Pneumonia | 99 (63.5) |
| Community-acquired | 68 (43.6) |
| Hospital-acquired | 31 (19.9) |
| Abdominal sepsis | 57 (36.5) |
| *Outcome* | |
| 28-day mortality | 48 (30.8) |
| 90-day mortality | 59 (37.8) |
| 1-year mortality | 77 (49.4) |

Data presented as median [Q1-Q3], or n (%).
Abbreviations: APACHE, Acute Physiology and Chronic Health Evaluation; ICU, Intensive care unit; GI, gastrointestinal; SOFA, Sequential Organ Failure Assessment.

## Figure legends

**Figure 1.** Coding and non-coding RNA expression in leukocytes of sepsis patients and healthy individuals. (**A**) Principal component (PC) plot depicting PC1 and PC2, and (**B**) the molecular distance to health (MDTH) index of protein-coding (n=18,063), long non-coding (n=16,087) and small non-coding RNAs (n=4949) in healthy subjects and sepsis patients. ** $p<0.01$; ***$p<0.001$. (**C**) Volcano plot representation of differences in coding and non-coding RNA expression between sepsis patients and healthy subjects. Horizontal (black) line denotes -log10 transformed adjusted p-value of 0.01. (**D**) Pie chart showing the subclass distribution of significant long non-coding RNA (adjusted $p < 0.01$). LincRNA, long intergenic non-coding RNA; rRNA, ribosomal RNA; TEC, To be Experimentally Confirmed; Mt tRNA, mitochondrial transfer RNA; Mt rRNA, mitochondrial ribosomal RNA. (**E**) Pie chart showing the subclass distribution of significant small non-coding RNA (adjusted $p < 0.01$). miRNA, microRNA; snoRNA, small nucleolar RNA; C/D box snoRNA, C/D box small mucleolar RNA; H/ACA box snoRNA, H/ACA box small mucleolar RNA; scaRNA, small cajal body-specific RNA.

**Figure 2**. Variance in coding and non-coding RNA expression attributed to demographics and clinical characteristics of sepsis patients. (**A**) Violin plots of percent variation in protein-coding, long and small non-coding RNA expression explained by sepsis patient demographics and clinical variables. Black dots depict outlier RNA transcripts. (**B**) Percent variance of select protein-coding and long non-coding RNA partitioned into the segment attributable to each demographic and clinical variable ranked by percent variation (>20%) for primary diagnosis (site of infection and place of acquisition). (**C**) Volcano plots depicting the changes in protein-coding and long non-coding RNA in patients discordant for septic shock on ICU admission. Horizontal (black) line denotes the adjusted p-value threshold for significance (adjusted $p \leq 0.01$).

Abbreviations: BC+, blood culture positive microbiology; diagnosis, infection site (lung or abdomen) and source (community or hospital); Charlson, Charlson comorbidity index; Apache IV, Acute Physiology and Chronic Health Evaluation; ICU, Intensive care unit; SOFA, Sequential Organ Failure Assessment.

**Figure 3**. Comparison of the coding and non-coding transcriptome in sepsis to human endotoxemia. (**A**) Dot plots depicting the correlation between protein-coding RNA fold expression indices in sepsis (compared to health) and fold expression after 2, 4, 6, 24 hours LPS infusion relative to pre-LPS. (**B**) Pie chart illustrating the biotypes of significantly altered long non-coding RNA (adjusted $p < 0.01$) across endotoxemia time points (2, 4, 6 and 24 hours after 2ng/kg lipopolysaccharide (LPS)). LincRNA, long intergenic non-coding RNA; rRNA, ribosomal RNA; TEC, To be Experimentally Confirmed; Mt tRNA, mitochondrial transfer RNA; Mt rRNA, mitochondrial ribosomal RNA. (**C**) Pie chart showing the biotypes of significantly altered small non-coding RNA (adjusted $p < 0.05$) in human endotoxemia. miRNA, microRNA; snoRNA, small nucleolar RNA; C/D box snoRNA, C/D box small mucleolar RNA; H/ACA box snoRNA, H/ACA box small mucleolar RNA; scaRNA, small cajal body-specific RNA. (**D**) Dot plots illustrating the correlation between long non-coding RNA fold expression indices in sepsis (compared to health) and fold expression of 2, 4, 6, 24 hours after LPS relative to pre-LPS. rho, Spearman's coefficient. (**E**) Dot plots depicting the correlation between small non-coding RNA fold expression indices in sepsis (compared to health) and 2, 4, 6, 24 hours after LPS relative to pre-LPS. rho, Spearman's coefficient.

**Figure 4**. Network analysis of coding and non-coding RNA expression. (**A**) Circular plot of protein-coding and long non-coding co-expression network modules characterized by

significantly associated (Fisher's adjusted $p < 0.01$) gene ontologies and Ingenuity canonical signaling pathways. Seventeen modules were associated to specific ontologies or canonical signaling pathways. (**B**) Bar plot depicting the distribution of protein coding and long non-coding RNA in each network module. * Fisher's Benjamini-Hochberg adjusted $p < 0.01$. (**C**) Dot plot illustrating the correlation between intramodular and total connectivities of each RNA transcript in their respective network module. Yellow dots illustrate protein-coding and long non-coding RNA in the RNA biosynthesis/RNA binding module; Turquoise dots depict the cell death and olfactory receptor activity module (**D**) Diagrammatic representation of Ingenuity's biofunctions (z-score<2 or >2 and adjusted $p < 0.05$) together with predicted long intergenic non-coding RNA (lincRNA) and antisense RNA in the cell death/olfactory receptor activity/cell-cycle G2/M DNA damage checkpoint and regulation module (turquoise). Blue, reduced expression; red, elevated expression in sepsis relative to health (fold change $\geq 1.2$ or $\leq -1.2$; adjusted p-value $< 0.01$). (**E**) Violin plots of network module eigengene (first principal component) percent variance attributable to small non-coding RNA.

**Figure 5**. <u>Relationship of protein-coding, non-coding RNA network modules to soluble mediators and clinical severity</u>. (**A**) Heatmap representation of Pearson correlation coefficients (adjusted $p < 0.05$) calculated for each network module eigengene (first principal component) against soluble mediators of inflammation, endothelial function, coagulation, as well as clinical parameters of disease severity. APACHE IV, Acute Physiology and Chronic Health Evaluation; SOFA, Sequential Organ Failure Assessment. Red denotes direct correlations and blue denotes indirect correlations (**B**) Boxplot showing differences in neutrophil degranulation (red) module eigengene values in sepsis patients discordant for septic shock on intensive care unit admission. High module eigengene values mean overall elevated RNA expression; low module eigengene

values mean reduced expression. (**C**) Diagrammatic representation of the neutrophil degranulation (secretory; red) module (Ingenuity's biofunction z-score<2 or >2; adjusted $p < 0.05$) together with predicted long intergenic non-coding RNA (lincRNA) and antisense RNA. Red or blue nodes denote high or low expression RNA transcripts in sepsis relative to health, respectively. *** Mann-Whitney $p<0.001$. (D and E) Dot plots of (D) *MYOSLID* expression and (E) *LUCAT1* expression against soluble mediators of inflammation IL-6, IL-8 and IL-10, as well as the acute phase response protein CRP. Rho, Spearman's coefficient.

## Supplementary File

### Patients

Comorbidities were defined as follows: Cardiovascular compromise was defined as a medical history of congestive heart failure, chronic cardiovascular disease, myocardial infarction, peripheral vascular disease or cerebrovascular disease. Malignancy was defined as a medical history of either metastatic or not metastatic solid tumor, or hemodynamic malignancy. Patients with a history of chronic renal insufficiency, or treated with chronic intermittent hemodialysis or continuous ambulatory peritoneal dialysis were marked as renal insufficient. Respiratory insufficiency included patients with a history of chronic respiratory insufficiency, chronic obstructive pulmonary disease, or treated at home with oxygen or ventilator support. Patients with a history of immune deficiency, human immunodeficiency virus (HIV) infection, acquired immune deficiency syndrome (AIDS), asplenia, or chronically treated with corticosteroids, antineoplastic or other immune suppressive medications were deemed immunocompromised.

Supplementary File Legends

**Supplementary File 1.** Table of causative pathogens in critically ill patients with sepsis (n=156). Percentages depict the proportion of infections caused by the pathogen indicated. In total, 192 pathogens were assigned to 156 infections. In 40 (25.6%) infections, more than one pathogen was assigned as causative.

**Figure 1 - figure supplement 1**. Ingenuity pathway analysis of significant protein-coding RNA in sepsis relative to health. Red bars denote pathways harboring protein-coding RNA with elevated expression; turquoise bars denote pathways harboring protein-coding RNA with reduced

expression. Significance was demarcated at Benjamini-Hochberg (BH) adjusted $p < 0.01$. -log(BH) p, negative log-transformed BH p-value.

**Figure 2 - figure supplement 1**. (**A**) Violin plots of percent variation in protein-coding, long and small non-coding RNA expression explained by age in gender in healthy subjects (n=82). Black dots depict outlier RNA. (**B**) Expression of long non-coding RNA *TXLNGY*, *LINC00278* and *XIST* in healthy males and females. (**C**) Volcano plot of significantly altered protein-coding RNA in non-survivors relative to survivors after 28 days since ICU admission. Horizontal (black) line denotes -log10 transformed adjusted p-value thresholds.

**Figure 3 - figure supplement 1. (A)** Volcano plot representation of significantly altered protein-coding RNA after 2, 4, 6 and 24 hours lipopolysaccharide (LPS) infusion relative to pre-LPS. Horizontal (black) line denotes -log10 transformed adjusted p-value threshold of 0.01. (**B-D**) Ingenuity pathway analysis of significant protein-coding RNA after 2, 4 and 6 hours human endotoxemia. Red bars denote pathways harboring protein-coding RNA with elevated expression; turquoise bars denote pathways harboring protein-coding RNA with reduced expression. Significance was demarcated at Benjamini-Hochberg (BH) adjusted $p < 0.01$. Adjusted P, negative log-transformed BH p-value.

**Figure 3 - figure supplement 2.** Volcano plot representations of significantly altered (**A**) long non-coding RNA and (**B**) small non-coding RNA after 2, 4, 6 and 24 hours lipopolysaccharide (LPS) relative to pre-LPS. Horizontal (black) line denotes -log10 transformed adjusted p-value thresholds.

**Figure 4 - figure supplement 1**. Co-expression network analysis. (**A**) Evaluation of scale free topology model fit and mean connectivities (y-axes) across various soft threshold powers (x-axis)

with scale independence denoted at $R^2 > 0.85$ (red horizontal line) for protein-coding and long non-coding RNA expression in sepsis patients (n=8539). (**B**) Topological overlap plot of adjacencies calculated for 8539 protein-coding and long non-coding RNA expression and module colors. (**C**) Cytoscape plot (organic layout) of protein-coding and long non-coding RNA (nodes) and connectivities (edges; weight > 0.2). Turquoise and yellow modules were visibly central to the co-expression network.

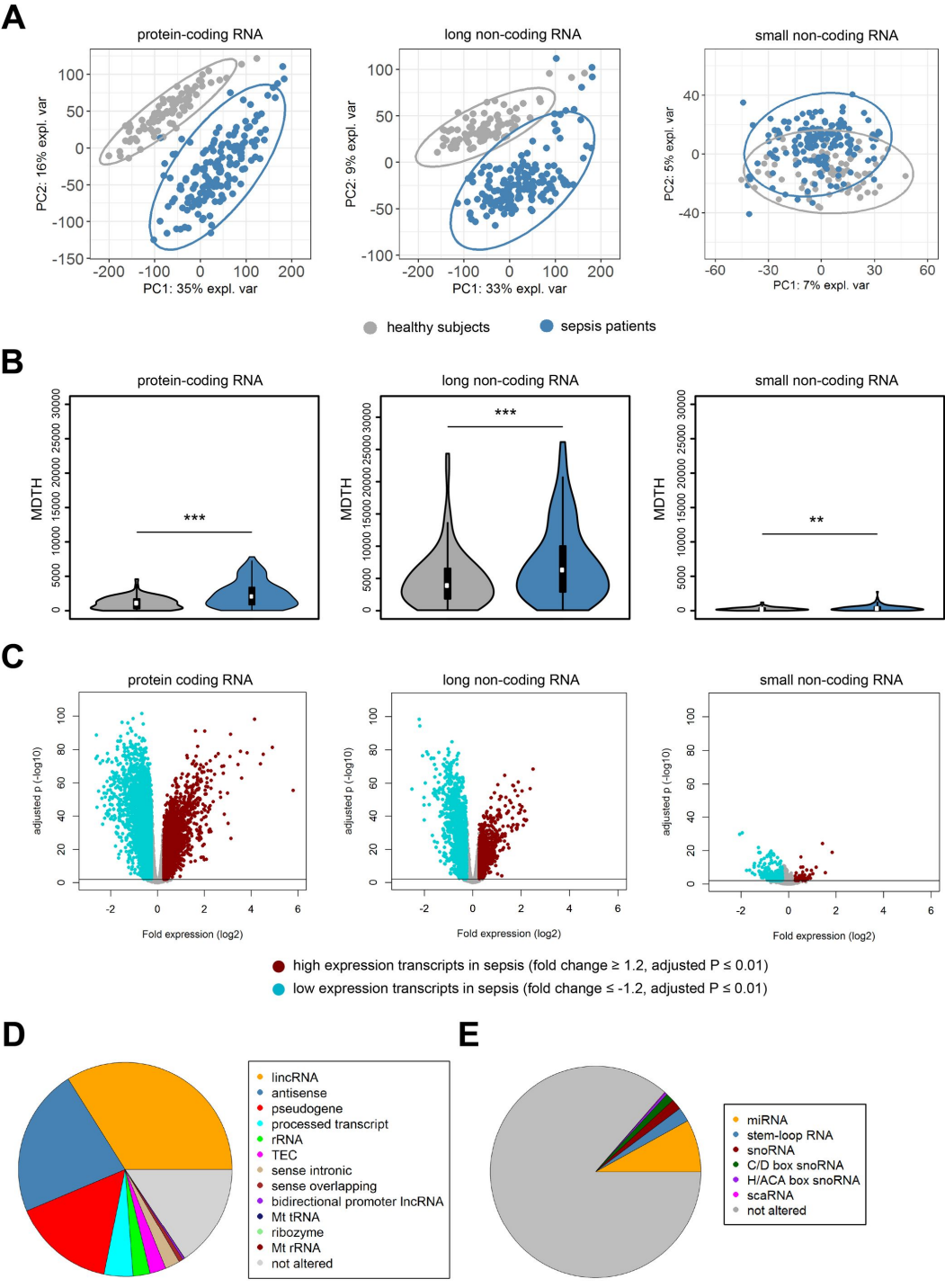
A
protein-coding RNA
long non-coding RNA
small non-coding RNA
PC2: 16% expl. var
PC1: 35% expl. var
PC2: 9% expl. var
PC1: 33% expl. var
PC2: 5% expl. var
PC1: 7% expl. var
healthy subjects
sepsis patients
B
protein-coding RNA
long non-coding RNA
small non-coding RNA
MDTH
***
***
**
C
protein coding RNA
long non-coding RNA
small non-coding RNA
adjusted p (-log10)
Fold expression (log2)
high expression transcripts in sepsis (fold change ≥ 1.2, adjusted P ≤ 0.01)
low expression transcripts in sepsis (fold change ≤ -1.2, adjusted P ≤ 0.01)
D
lincRNA
antisense
pseudogene
processed transcript
rRNA
TEC
sense intronic
sense overlapping
bidirectional promoter lncRNA
Mt tRNA
ribozyme
Mt rRNA
not altered
E
miRNA
stem-loop RNA
snoRNA
C/D box snoRNA
H/ACA box snoRNA
scaRNA
not altered

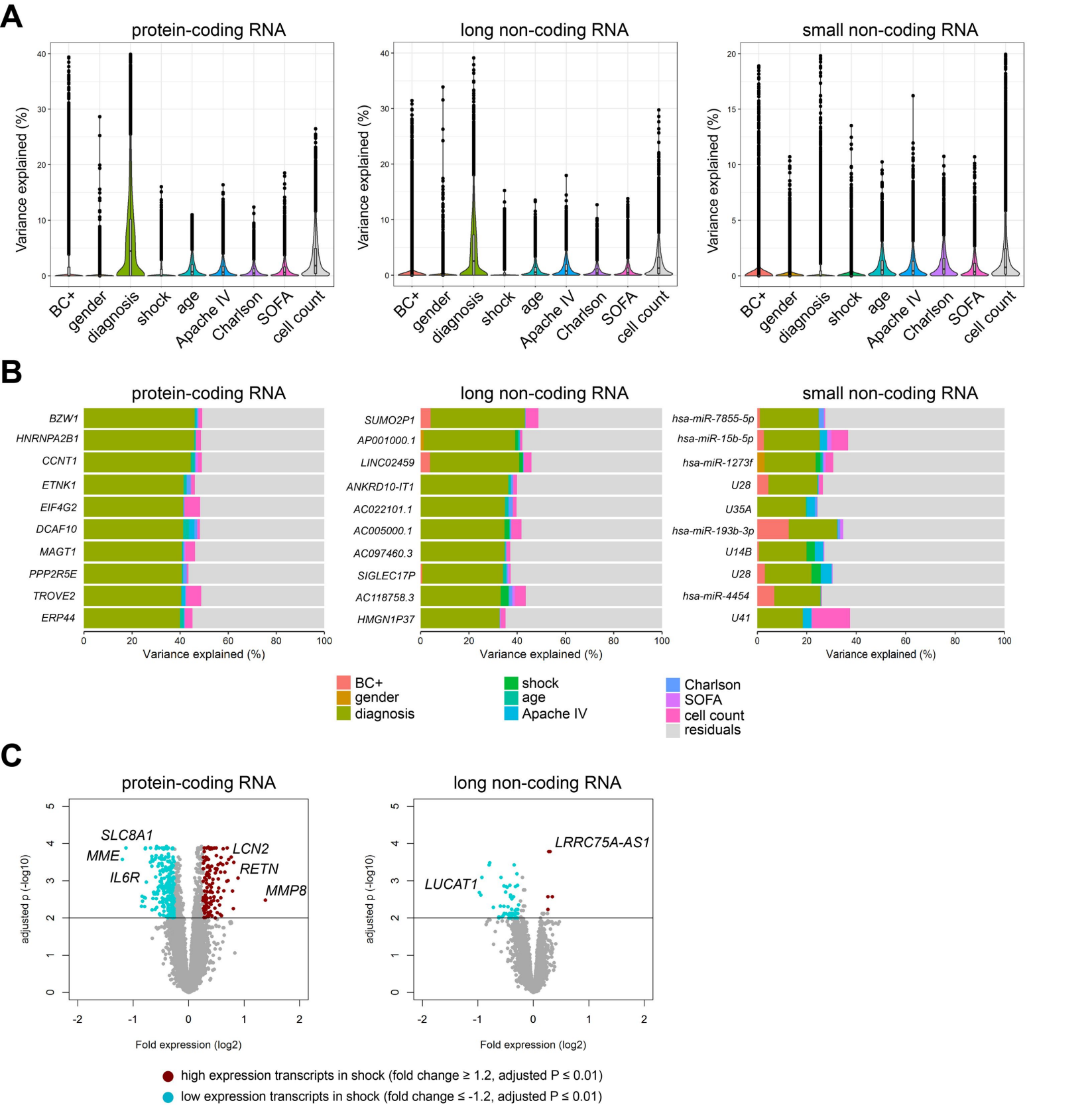
A
protein-coding RNA
long non-coding RNA
small non-coding RNA
Variance explained (%)
BC+
gender
diagnosis
shock
age
Apache IV
Charlson
SOFA
cell count
B
protein-coding RNA
long non-coding RNA
small non-coding RNA
BZW1
HNRNPA2B1
CCNT1
ETNK1
EIF4G2
DCAF10
MAGT1
PPP2R5E
TROVE2
ERP44
SUMO2P1
AP001000.1
LINC02459
ANKRD10-IT1
AC022101.1
AC005000.1
AC097460.3
SIGLEC17P
AC118758.3
HMGN1P37
hsa-miR-7855-5p
hsa-miR-15b-5p
hsa-miR-1273f
U28
U35A
hsa-miR-193b-3p
U14B
U28
hsa-miR-4454
U41
Variance explained (%)
BC+
gender
diagnosis
shock
age
Apache IV
Charlson
SOFA
cell count
residuals
C
protein-coding RNA
long non-coding RNA
SLC8A1
MME
IL6R
LCN2
RETN
MMP8
LRRC75A-AS1
LUCAT1
adjusted p (-log10)
Fold expression (log2)
high expression transcripts in shock (fold change ≥ 1.2, adjusted P ≤ 0.01)
low expression transcripts in shock (fold change ≤ -1.2, adjusted P ≤ 0.01)

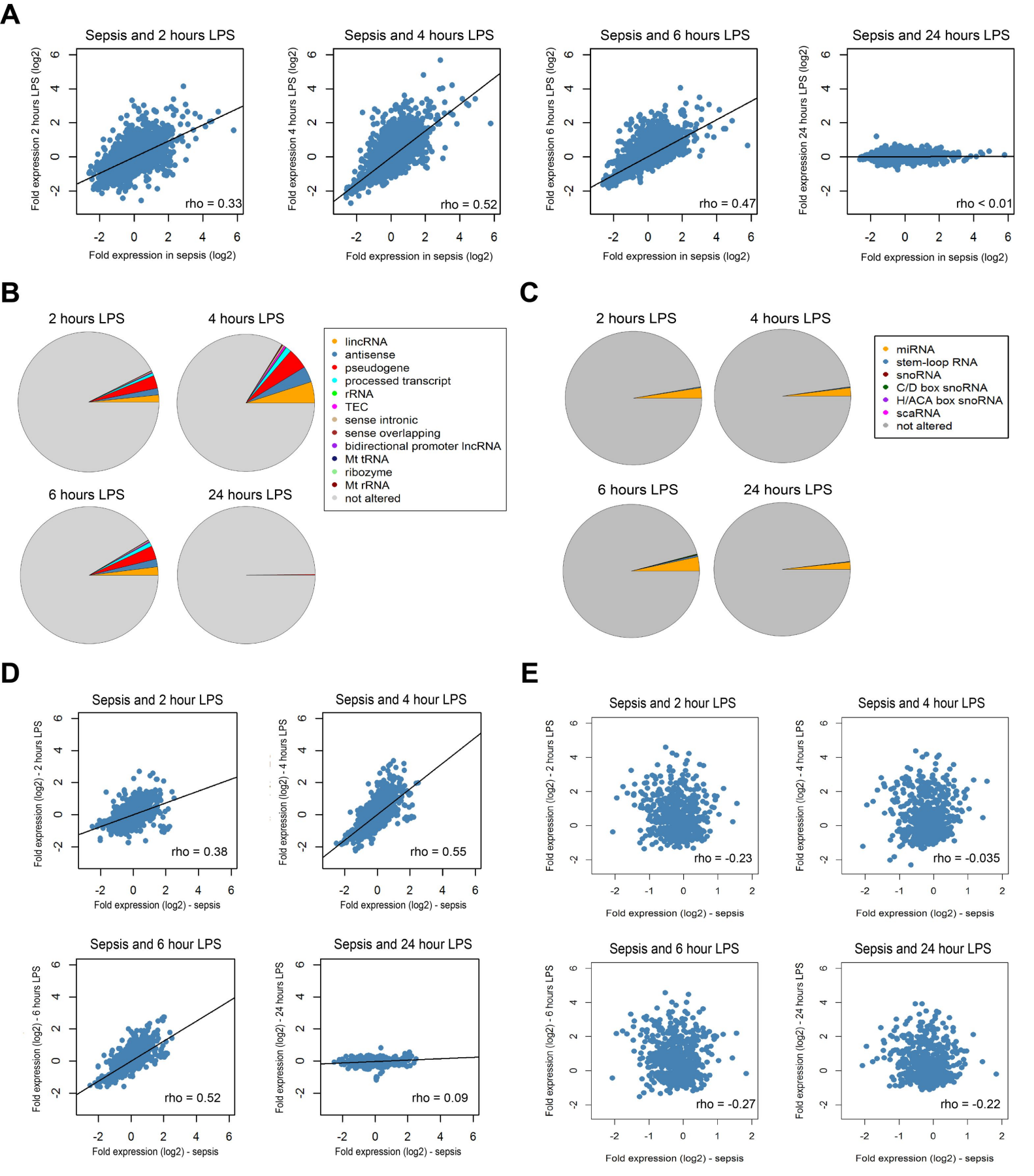
A
Sepsis and 2 hours LPS
Fold expression 2 hours LPS (log2)
rho = 0.33
Sepsis and 4 hours LPS
Fold expression 4 hours LPS (log2)
rho = 0.52
Sepsis and 6 hours LPS
Fold expression 6 hours LPS (log2)
rho = 0.47
Sepsis and 24 hours LPS
Fold expression 24 hours LPS (log2)
rho < 0.01
Fold expression in sepsis (log2)
B
2 hours LPS
4 hours LPS
6 hours LPS
24 hours LPS
lincRNA
antisense
pseudogene
processed transcript
rRNA
TEC
sense intronic
sense overlapping
bidirectional promoter lncRNA
Mt tRNA
ribozyme
Mt rRNA
not altered
C
2 hours LPS
4 hours LPS
6 hours LPS
24 hours LPS
miRNA
stem-loop RNA
snoRNA
C/D box snoRNA
H/ACA box snoRNA
scaRNA
not altered
D
Sepsis and 2 hour LPS
Fold expression (log2) - 2 hours LPS
rho = 0.38
Sepsis and 4 hour LPS
Fold expression (log2) - 4 hours LPS
rho = 0.55
Sepsis and 6 hour LPS
Fold expression (log2) - 6 hours LPS
rho = 0.52
Sepsis and 24 hour LPS
Fold expression (log2) - 24 hours LPS
rho = 0.09
Fold expression (log2) - sepsis
E
Sepsis and 2 hour LPS
Fold expression (log2) - 2 hours LPS
rho = -0.23
Sepsis and 4 hour LPS
Fold expression (log2) - 4 hours LPS
rho = -0.035
Sepsis and 6 hour LPS
Fold expression (log2) - 6 hours LPS
rho = -0.27
Sepsis and 24 hour LPS
Fold expression (log2) - 24 hours LPS
rho = -0.22
Fold expression (log2) - sepsis

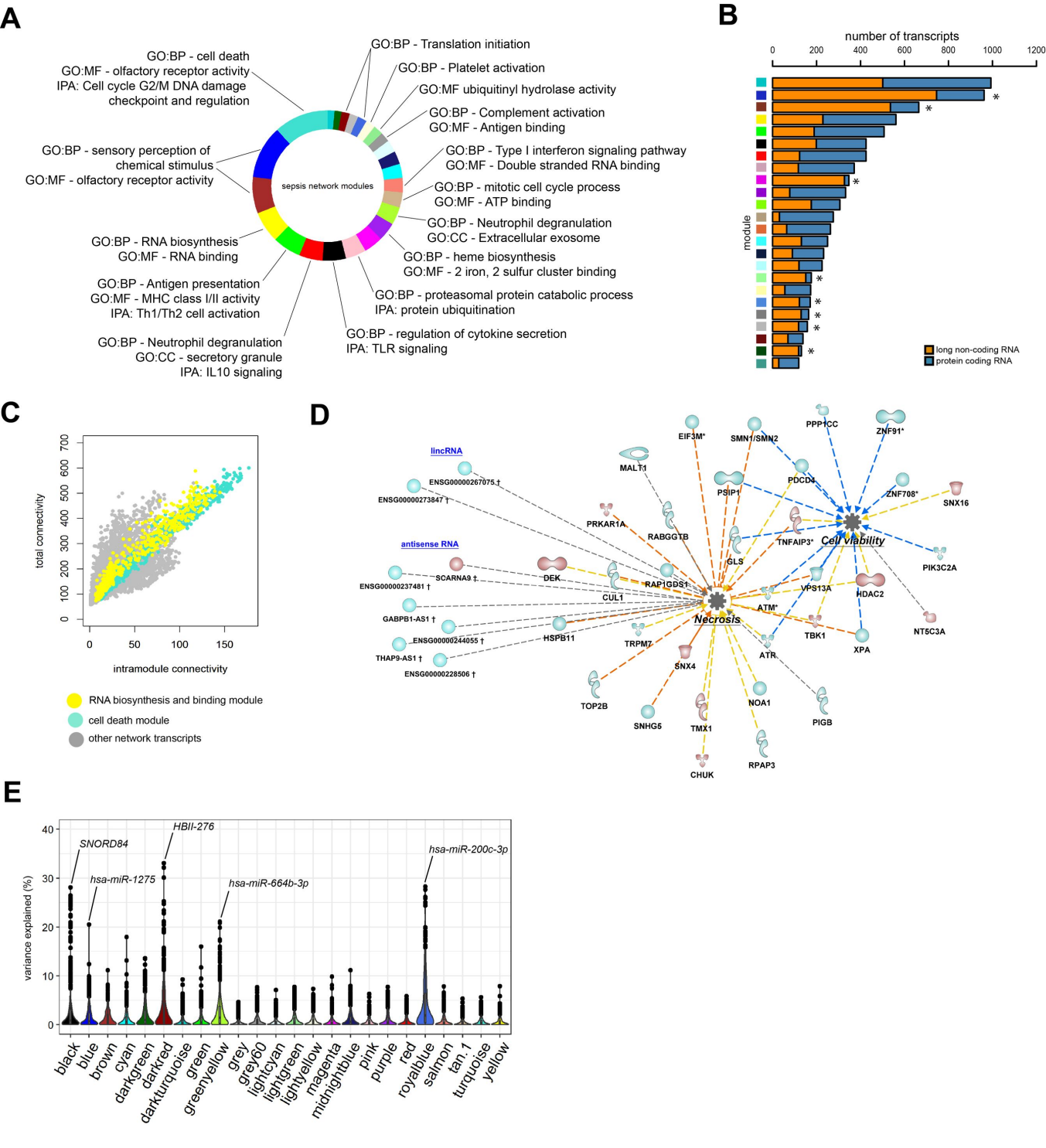
A
sepsis network modules
GO:BP - cell death
GO:MF - olfactory receptor activity
IPA: Cell cycle G2/M DNA damage checkpoint and regulation
GO:BP - sensory perception of chemical stimulus
GO:MF - olfactory receptor activity
GO:BP - RNA biosynthesis
GO:MF - RNA binding
GO:BP - Antigen presentation
GO:MF - MHC class I/II activity
IPA: Th1/Th2 cell activation
GO:BP - Neutrophil degranulation
GO:CC - secretory granule
IPA: IL10 signaling
GO:BP - regulation of cytokine secretion
IPA: TLR signaling
GO:BP - proteasomal protein catabolic process
IPA: protein ubiquitination
GO:BP - heme biosynthesis
GO:MF - 2 iron, 2 sulfur cluster binding
GO:BP - Neutrophil degranulation
GO:CC - Extracellular exosome
GO:BP - mitotic cell cycle process
GO:MF - ATP binding
GO:BP - Type I interferon signaling pathway
GO:MF - Double stranded RNA binding
GO:BP - Complement activation
GO:MF - Antigen binding
GO:MF ubiquitinyl hydrolase activity
GO:BP - Platelet activation
GO:BP - Translation initiation
B
number of transcripts
0
200
400
600
800
1000
1200
module
long non-coding RNA
protein coding RNA
C
total connectivity
0
100
200
300
400
500
600
700
intramodule connectivity
0
50
100
150
RNA biosynthesis and binding module
cell death module
other network transcripts
D
lincRNA
ENSG00000267075 †
ENSG00000273847 †
antisense RNA
SCARNA9 †
ENSG00000237481 †
GABPB1-AS1 †
ENSG00000244055 †
THAP9-AS1 †
ENSG00000228506 †
MALT1
PRKAR1A
RABGGTB
DEK
CUL1
RAP1GDS1
HSPB11
TRPM7
SNX4
TOP2B
SNHG5
TMX1
CHUK
RPAP3
NOA1
PIGB
EIF3M*
SMN1/SMN2
PSIP1
GLS
PPP1CC
ZNF91*
PDCD4
ZNF708*
SNX16
TNFAIP3*
Cell Viability
PIK3C2A
VPS13A
HDAC2
ATM*
Necrosis
TBK1
NT5C3A
ATR
XPA
E
variance explained (%)
0
10
20
30
40
SNORD84
hsa-miR-1275
HBII-276
hsa-miR-664b-3p
hsa-miR-200c-3p
black
blue
brown
cyan
darkgreen
darkred
darkturquoise
green
greenyellow
grey
grey60
lightcyan
lightgreen
lightyellow
magenta
midnightblue
pink
purple
red
royalblue
salmon
tan_1
turquoise
yellow

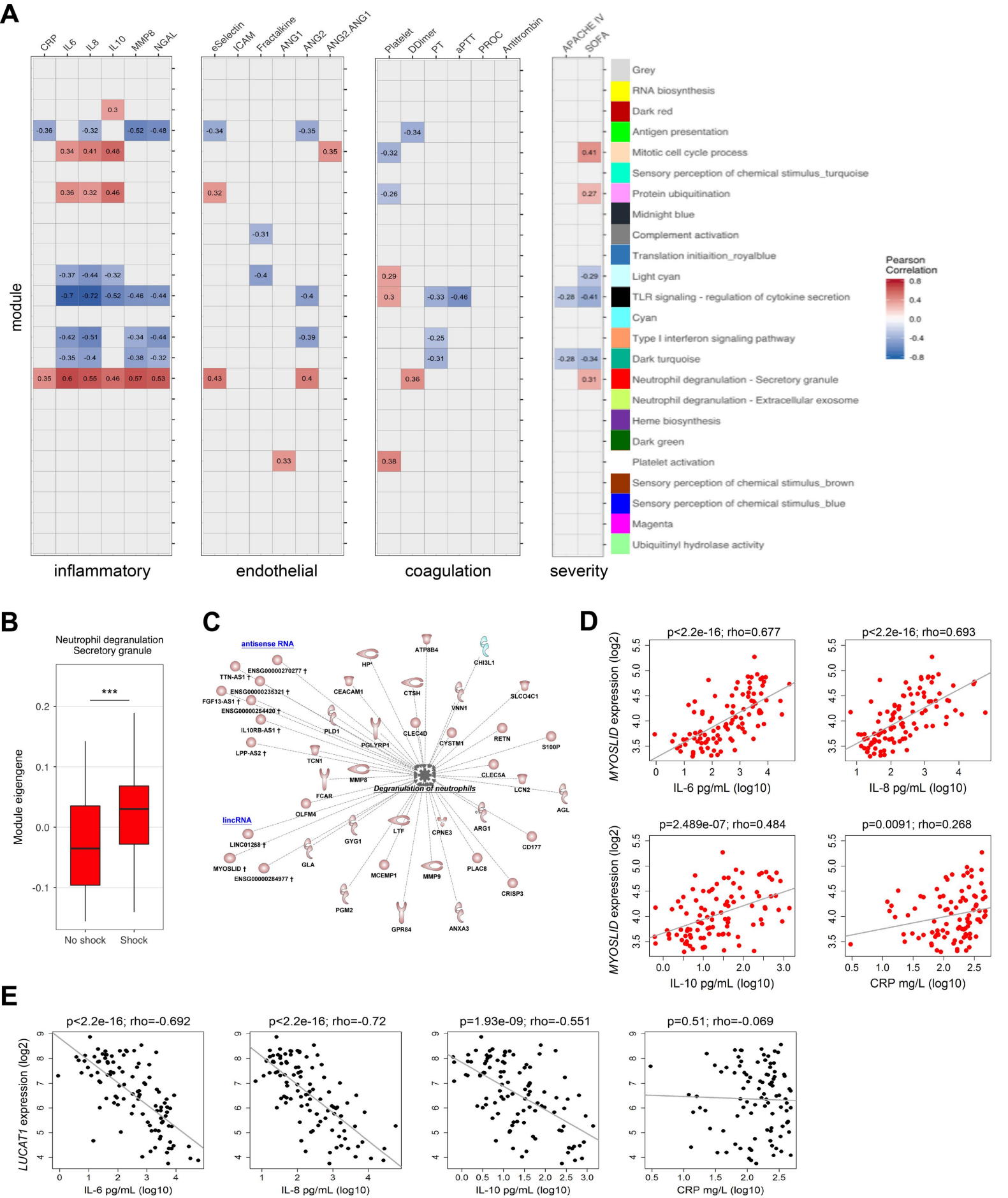
A
CRP
IL6
IL8
IL10
MMP8
NGAL
eSelectin
ICAM
Fractalkine
ANG1
ANG2
ANG2.ANG1
Platelet
DDimer
PT
aPTT
PROC
Antithrombin
APACHE IV
SOFA
module
Grey
RNA biosynthesis
Dark red
Antigen presentation
Mitotic cell cycle process
Sensory perception of chemical stimulus_turquoise
Protein ubiquitination
Midnight blue
Complement activation
Translation initiaition_royalblue
Light cyan
TLR signaling - regulation of cytokine secretion
Cyan
Type I interferon signaling pathway
Dark turquoise
Neutrophil degranulation - Secretory granule
Neutrophil degranulation - Extracellular exosome
Heme biosynthesis
Dark green
Platelet activation
Sensory perception of chemical stimulus_brown
Sensory perception of chemical stimulus_blue
Magenta
Ubiquitinyl hydrolase activity
Pearson Correlation
0.8
0.4
0.0
-0.4
-0.8
inflammatory
endothelial
coagulation
severity
B
Neutrophil degranulation
Secretory granule
***
Module eigengene
No shock
Shock
C
antisense RNA
lincRNA
Degranulation of neutrophils
D
p<2.2e-16; rho=0.677
p<2.2e-16; rho=0.693
p=2.489e-07; rho=0.484
p=0.0091; rho=0.268
MYOSLID expression (log2)
IL-6 pg/mL (log10)
IL-8 pg/mL (log10)
IL-10 pg/mL (log10)
CRP mg/L (log10)
E
p<2.2e-16; rho=-0.692
p<2.2e-16; rho=-0.72
p=1.93e-09; rho=-0.551
p=0.51; rho=-0.069
LUCAT1 expression (log2)
IL-6 pg/mL (log10)
IL-8 pg/mL (log10)
IL-10 pg/mL (log10)
CRP mg/L (log10)

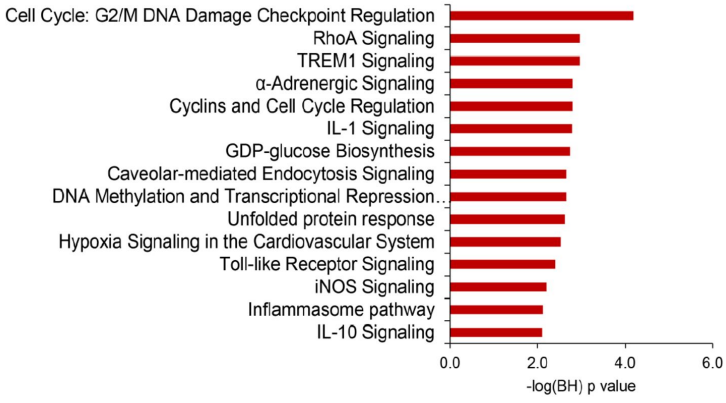
Cell Cycle: G2/M DNA Damage Checkpoint Regulation
RhoA Signaling
TREM1 Signaling
α-Adrenergic Signaling
Cyclins and Cell Cycle Regulation
IL-1 Signaling
GDP-glucose Biosynthesis
Caveolar-mediated Endocytosis Signaling
DNA Methylation and Transcriptional Repression...
Unfolded protein response
Hypoxia Signaling in the Cardiovascular System
Toll-like Receptor Signaling
iNOS Signaling
Inflammasome pathway
IL-10 Signaling
0.0
2.0
4.0
6.0
-log(BH) p value

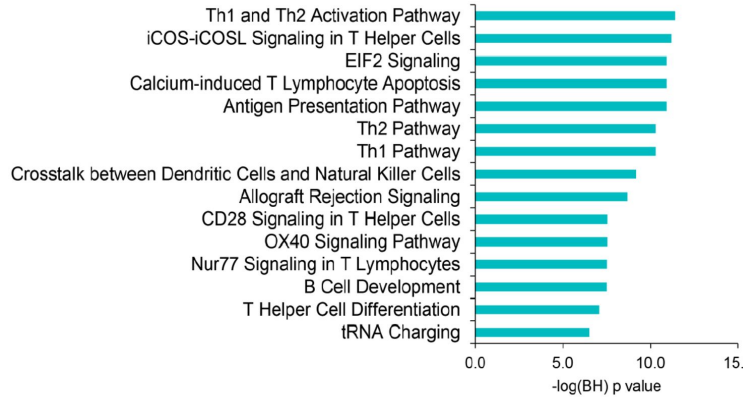
Th1 and Th2 Activation Pathway
iCOS-iCOSL Signaling in T Helper Cells
EIF2 Signaling
Calcium-induced T Lymphocyte Apoptosis
Antigen Presentation Pathway
Th2 Pathway
Th1 Pathway
Crosstalk between Dendritic Cells and Natural Killer Cells
Allograft Rejection Signaling
CD28 Signaling in T Helper Cells
OX40 Signaling Pathway
Nur77 Signaling in T Lymphocytes
B Cell Development
T Helper Cell Differentiation
tRNA Charging
0.0
5.0
10.0
15.0
-log(BH) p value

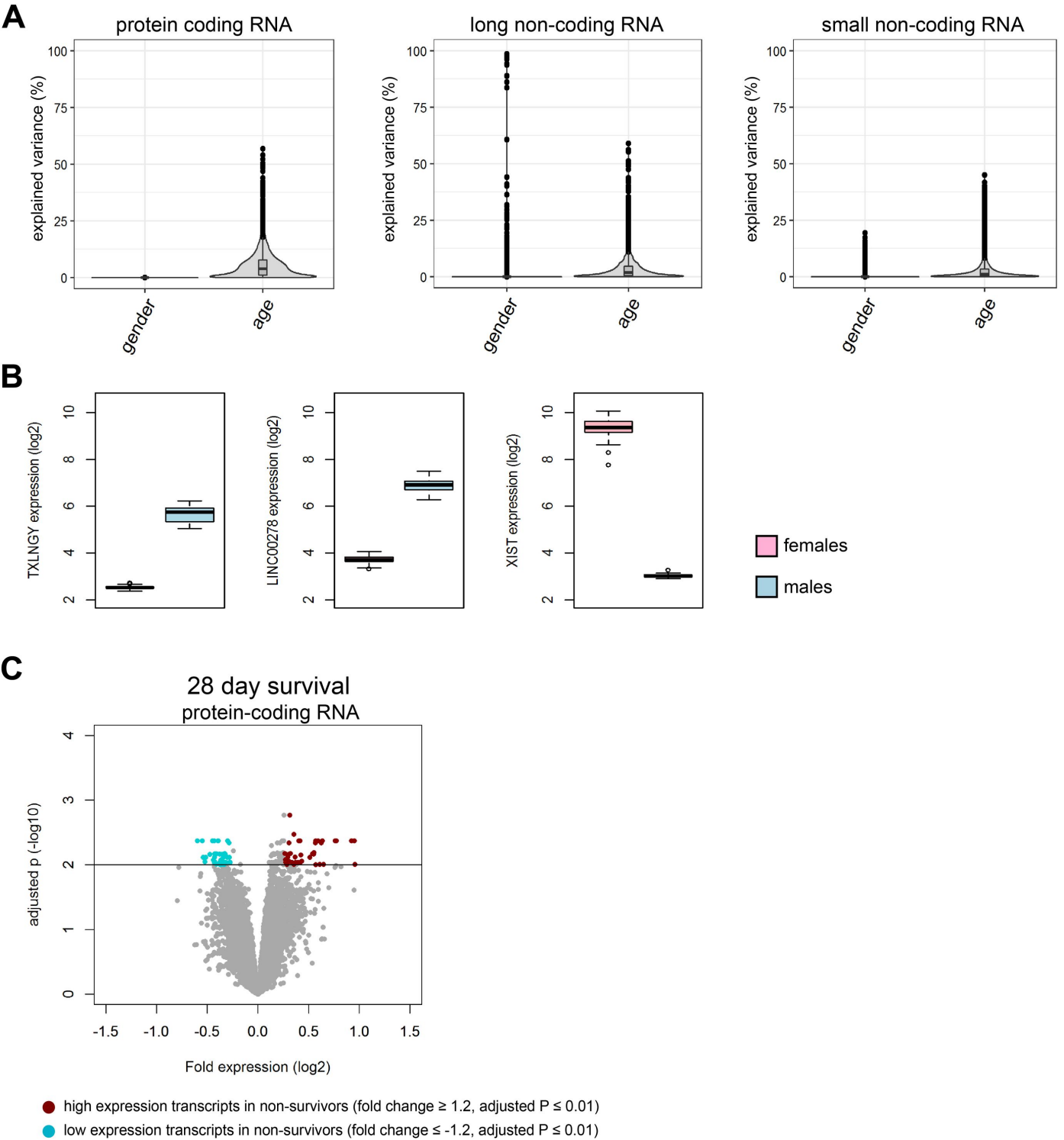
A
protein coding RNA
long non-coding RNA
small non-coding RNA
explained variance (%)
100
75
50
25
0
gender
age
B
TXLNGY expression (log2)
LINC00278 expression (log2)
XIST expression (log2)
2
4
6
8
10
females
males
C
28 day survival
protein-coding RNA
adjusted p (-log10)
0
1
2
3
4
-1.5
-1.0
-0.5
0.0
0.5
1.0
1.5
Fold expression (log2)
high expression transcripts in non-survivors (fold change ≥ 1.2, adjusted P ≤ 0.01)
low expression transcripts in non-survivors (fold change ≤ -1.2, adjusted P ≤ 0.01)

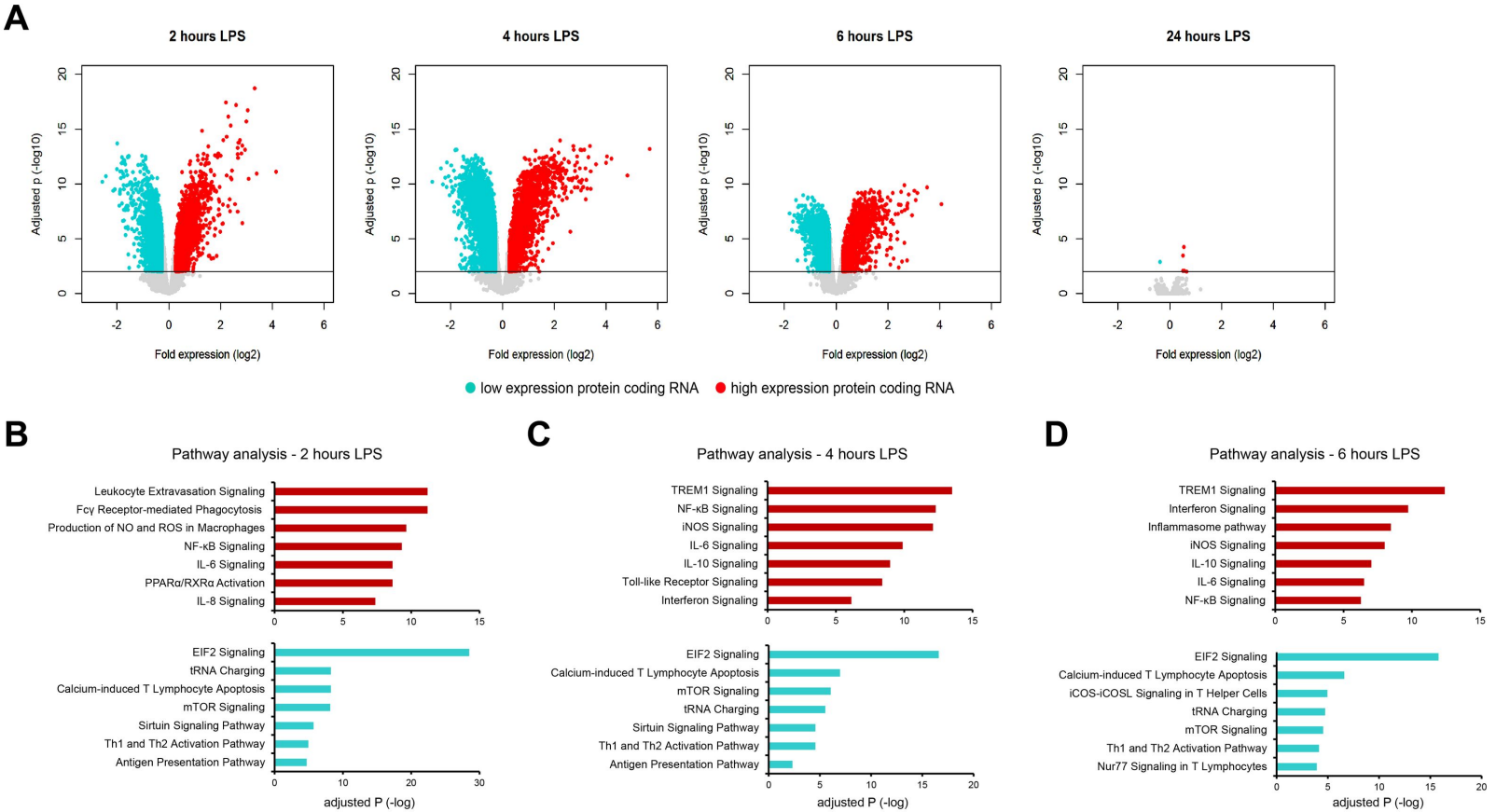
A
2 hours LPS
4 hours LPS
6 hours LPS
24 hours LPS
Adjusted p (-log10)
Fold expression (log2)
low expression protein coding RNA
high expression protein coding RNA
B
Pathway analysis - 2 hours LPS
Leukocyte Extravasation Signaling
Fcγ Receptor-mediated Phagocytosis
Production of NO and ROS in Macrophages
NF-κB Signaling
IL-6 Signaling
PPARα/RXRα Activation
IL-8 Signaling
EIF2 Signaling
tRNA Charging
Calcium-induced T Lymphocyte Apoptosis
mTOR Signaling
Sirtuin Signaling Pathway
Th1 and Th2 Activation Pathway
Antigen Presentation Pathway
adjusted P (-log)
C
Pathway analysis - 4 hours LPS
TREM1 Signaling
NF-κB Signaling
iNOS Signaling
IL-6 Signaling
IL-10 Signaling
Toll-like Receptor Signaling
Interferon Signaling
EIF2 Signaling
Calcium-induced T Lymphocyte Apoptosis
mTOR Signaling
tRNA Charging
Sirtuin Signaling Pathway
Th1 and Th2 Activation Pathway
Antigen Presentation Pathway
adjusted P (-log)
D
Pathway analysis - 6 hours LPS
TREM1 Signaling
Interferon Signaling
Inflammasome pathway
iNOS Signaling
IL-10 Signaling
IL-6 Signaling
NF-κB Signaling
EIF2 Signaling
Calcium-induced T Lymphocyte Apoptosis
iCOS-iCOSL Signaling in T Helper Cells
tRNA Charging
mTOR Signaling
Th1 and Th2 Activation Pathway
Nur77 Signaling in T Lymphocytes
adjusted P (-log)

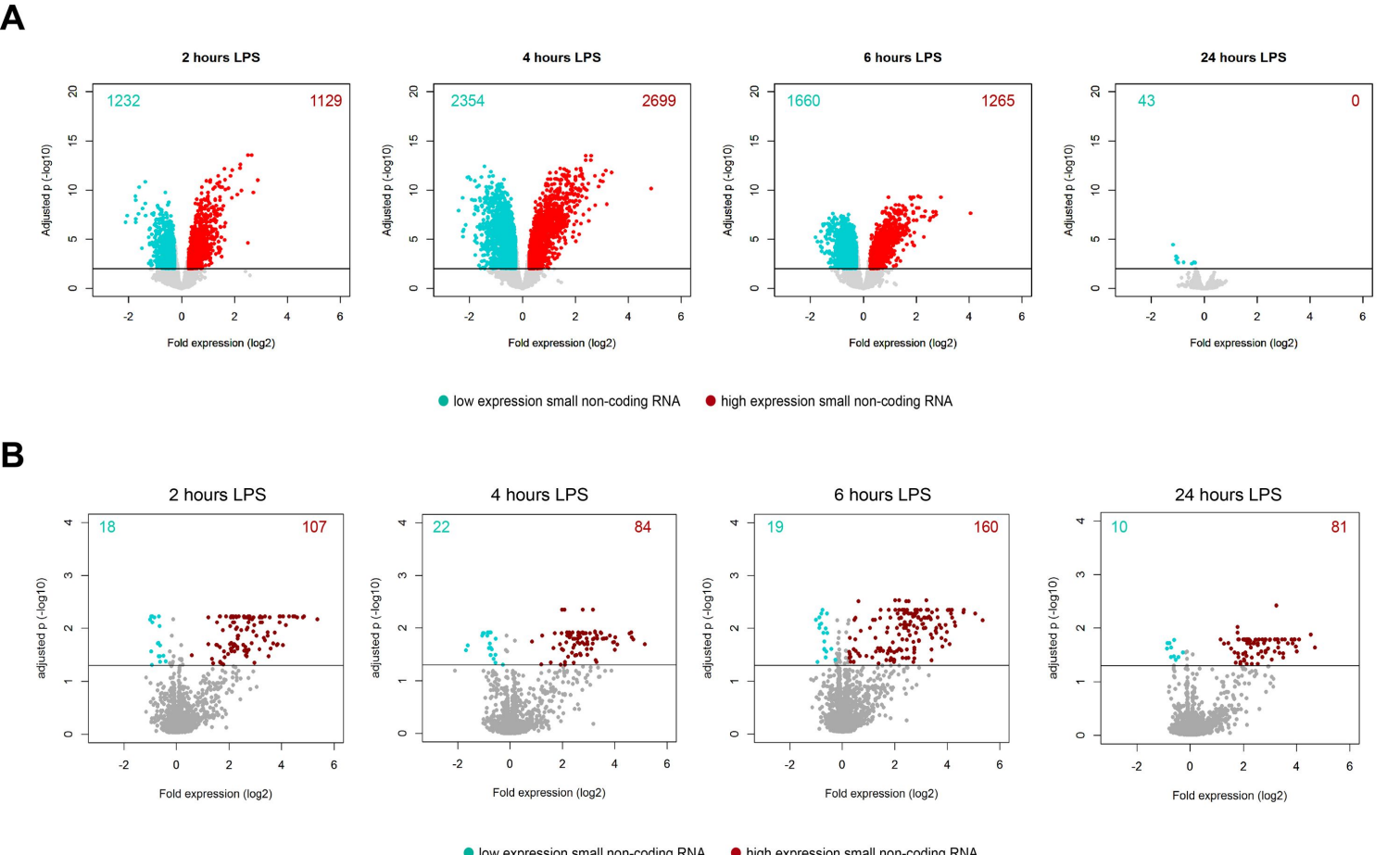
A
2 hours LPS
1232
1129
4 hours LPS
2354
2699
6 hours LPS
1660
1265
24 hours LPS
43
0
Adjusted p (-log10)
Fold expression (log2)
low expression small non-coding RNA
high expression small non-coding RNA
B
2 hours LPS
18
107
4 hours LPS
22
84
6 hours LPS
19
160
24 hours LPS
10
81
adjusted p (-log10)
Fold expression (log2)
low expression small non-coding RNA
high expression small non-coding RNA

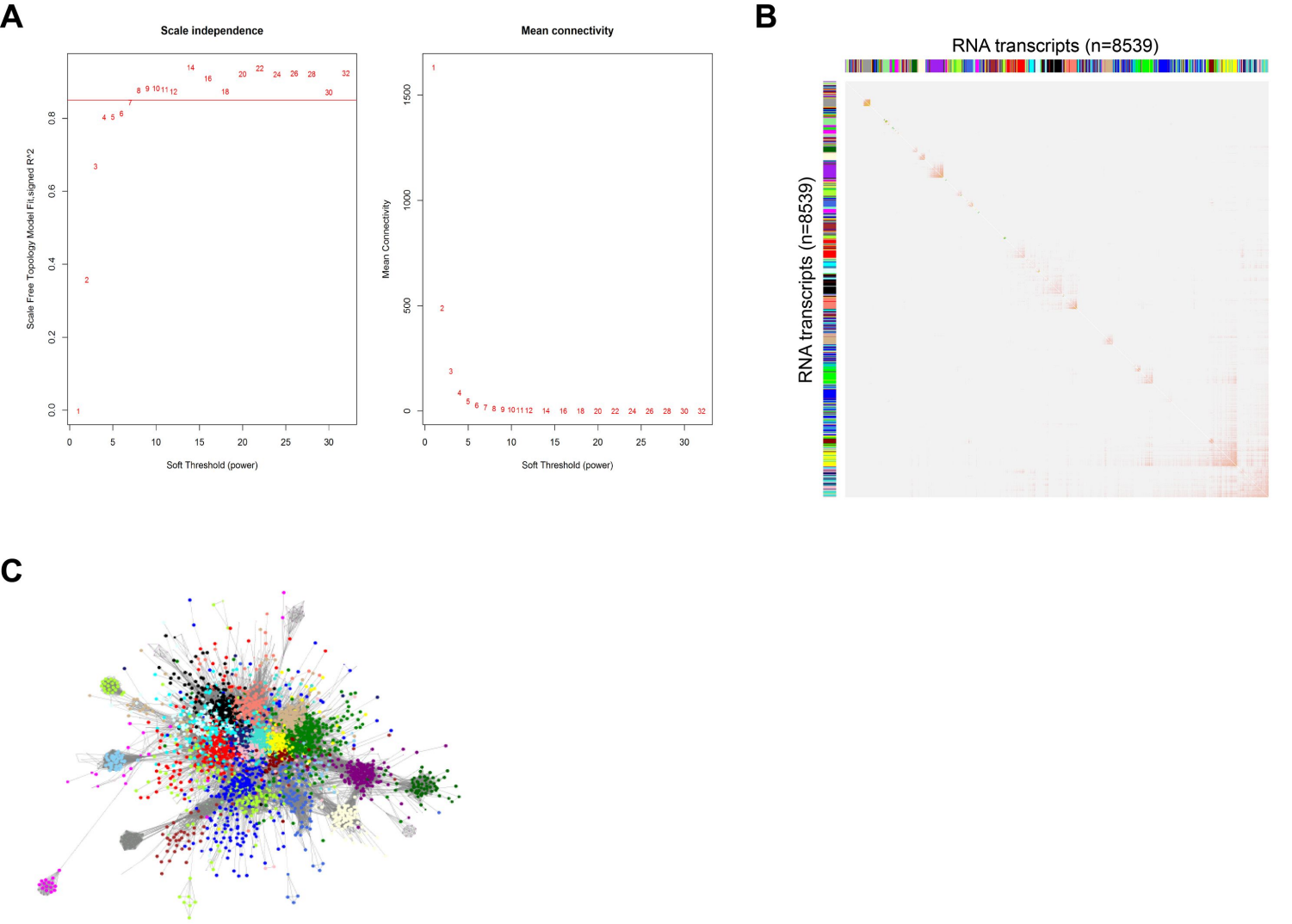
A
Scale independence
Scale Free Topology Model Fit,signed R^2
Soft Threshold (power)
Mean connectivity
Mean Connectivity
Soft Threshold (power)
B
RNA transcripts (n=8539)
RNA transcripts (n=8539)
C